2(mix)

ELECTRICAL

ENGINEERING

ENGINEERING EXPERIMENT STATION

AUBURN UNIVERSITY

AUBURN, ALABAMA

FINAL REPORT

VOLUME 2

TELEVISION BROADCAST RELAY SYSTEM

Prepared By

SATELLITE COMMUNICATIONS LABORATORY

E. R. GRAF, PROJECT LEADER

CR-123909

Contract NAS8-24818
GEORGE C. MARSHALL SPACE FLIGHT CENTER
NATIONAL AERONAUTICS AND SPACE ADMINISTRATION
HUNTSVILLE, ALABAMA

Approved By: Submitted By:

C. C. Carroll   E. R. Graf
Professor and Head   Professor
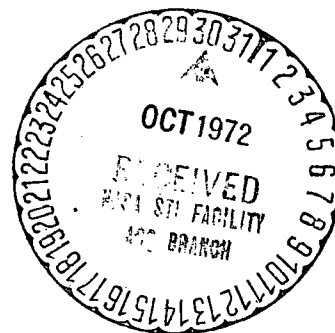Electrical Engineering   Electrical Engineering

FINAL REPORT

VOLUME 2

TELEVISION BROADCAST RELAY SYSTEM

Prepared By

SATELLITE COMMUNICATIONS LABORATORY

E. R. GRAF, PROJECT LEADER

Contract NAS8-24818
GEORGE C. MARSHALL SPACE FLIGHT CENTER
NATIONAL AERONAUTICS AND SPACE ADMINISTRATION
HUNTSVILLE, ALABAMA

Approved By: Submitted By:

C. C. Carroll   E. R. Graf
Professor and Head   Professor
Electrical Engineering   Electrical Engineering

i

FOREWORD

This report is a Technical summary presenting the results of a study by the Satellite Communications Laboratory of the Electrical Engineering Department, Auburn University, under the auspices of the Engineering Experiment Station. The report is submitted in partial fulfillment of the requirements in NASA contract number NAS8-24818.

ACKNOWLEDGEMENT

ABSTRACT

DETERMINATION OF CONTOURS OF PICTURE

QUALITY FOR SATELLITE TELEVISION

BROADCASTING SYSTEMS

S. G. CHANDRASEKHARAIAH

Final Report
Contract NAS8-24818
prepared by
Satellite Communications Laboratory
E. R. Graf, Project Leader
June 1972

The inevitable rise of domestic communication satellites has already

begun with the "molniya" system successfully operating in the U.S.S.R.

and another system "Anik" to be implemented in Canada. Also the present

review of U. S. domestic proposals by the FCC heralds a totally new con-

cept of communications. It has generally been agreed that the Television

Broadcast Satellite (TVBS) has the greatest potential for directly

helping the peoples of the world. Extremely careful planning is needed

in the design of these systems, because of the high initial cost

involved.

The space frequencies that are allocated for broadcasting are in

the 2.5 GHz and 12 GHz range. Though ionospheric effects are negligible

at these frequencies, tropospheric effects become important, especially

at 12 GHz. Further, these effects are highly weather dependent and

statistical analysis is needed for an optimum system design. Hence by using climatological data for one year and for different locations in the U. S., the time and location probability data of the atmospheric attenuation and sky noise temperature have been determined in the present work. These are presented in the most general form so as to be applicable to any satellite communication system design for the temperate regions of the world.

Further a method has been derived to obtain picture quality contours for a given system and coverage area of the earth. The method is highly flexible and a number of alternative factors may be considered for an optimum design of any system.

TABLE OF CONTENTS

LIST OF TABLES

LIST OF FIGURES

x

I. INTRODUCTION

The Television Systems around the world have seen a very rapid
growth in the last few years. The effects of television have been
numerous. Most of the countries have adopted television not only for
entertainment and educational purposes but also as a means to achieve
national unity. The most important problem in any country, is that of
insuring a good ground coverage of the broadcasting signals so that the
percentage of homes which can receive television without complex aerials
or amplyfying equipment approaches 100%. At the present time, to
achieve close to 100% coverage with ground links requires a very large
number of conventional transmitting stations and the increase in dis-
tribution costs to achieve this coverage may be very much higher than
the increased revenue that would result.

The most attractive alternate to this is the possibility of using
space technology to provide television broadcast signals to the required
areas of earth. Of all the applications of today's space program, the
Television Broadcast Satellite (TVBS) probably has the greatest potential
for directly helping the peoples of the world. Many technical feasibility
studies of the Satellite Communication Systems [1 through 13] have been
made. The economical, educational and other aspects of such systems
have also been widely discussed [14 through 17]. It has been generally
agreed that the TVBS, in its various forms, can provide mass communication

1

and education where there are none; it can extend and improve them where they exist; and it can accomplish these services more cheaply and quickly than any other means.

The first domestic communication satellite in America, 'TELESAT' is now being designed to augment the international Communications Systems of Canada. This Synchronous Satellite is scheduled for launch by NASA at the end of 1972. [18, 19, and 20].

The term 'Television by Satellite' is open to many interpretations, of which the most extreme in technical difficulty is the case of the Direct Television broadcaster, that is to say, a Satellite transmitting directly into home receivers. Past and present television communication by satellites has been limited to relaying to large, complex ground receiving terminals. Satellites for this type of existing service operate at very low levels of RF power output and low transmitting antenna gain. The current technological state of the art is adequate for the small, low-cost satellite of this type, a fact which has been demonstrated. However, for direct broadcasting, high power broadcast satellites are required for transmission to thousands of receiving terminals, which must essentially be low cost receivers. Various studies have resulted in the conclusion that if the current technology and subsystem development is continued, high power spaceborne TV transmitters and low cost receivers are feasible in the 1970-1985 period [21].

A typical Synchronous Satellite System configuration is shown in Figure 1. A ground transmitting station for each channel beams its output to a geo-stationary satellite and the satellite responder relays the signals directly to the home receiver (or to the community antenna terminal). A geo-stationary satellite (altitude about 35,200 km above the equator) would permit a continuous 24 hour broadcast service to the area of coverage required.

A primary design objective for a TVBS system is to provide the required quality signal by the most economical method - economical in both dollar cost and frequency spectrum conservation. Among the parameters that must be considered in designing a TVBS system are:

Television standards and signal formats

Subjective picture quality

Type of modulation

Sound channel requirements

Propagation factors

Man-made noise

Satellite subsystem technology limitations

Receiving terminal cost and complexity limitations.

In this study, propagation factors are discussed in detail and their effect on the subjective picture quality has been investigated. CCIR has allocated space frequencies of 2.50 - 2.69 GHz for Instructional Services and 11.7 - 12.2 GHz for Broadcasting. Hence frequencies of
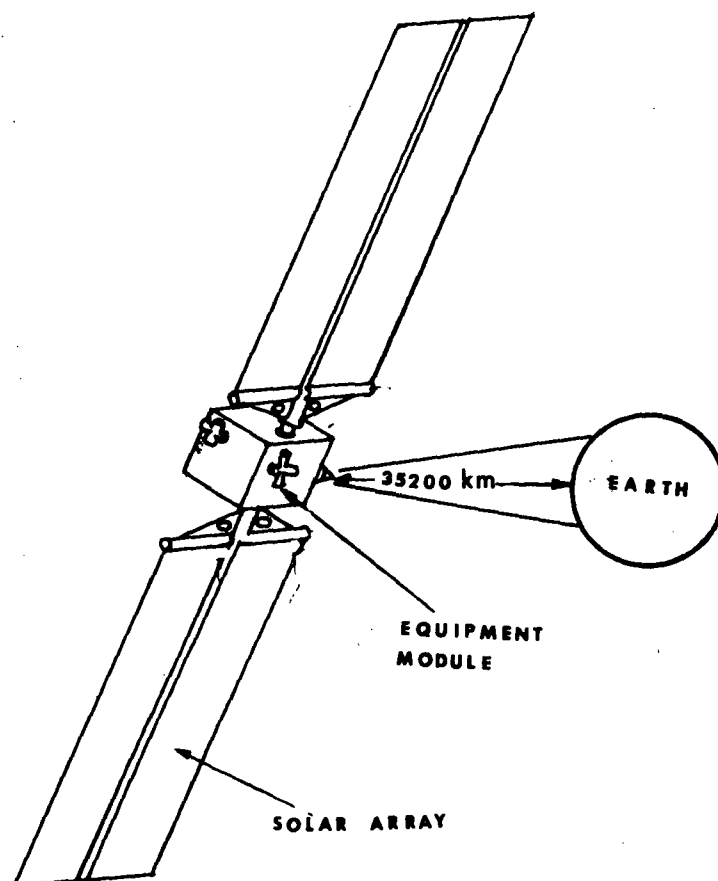
Figure 1. Synchronous Satellite Configuration.

2.5 GHz and 12 GHz are considered in this study. Only frequency modulation need be considered because of lower transmitter power requirements.

Subjective picture quality was the subject of extensive investigations by the Television Allocation Study Organization (TASO) during 1959-60. In their final report [22], the level of television service has been characterized by specifying

(1) the signal carrier-to-noise ratio required for a given picture quality to be achieved or exceeded, and

(2) the time and location probabilities of receiving at least that level of picture quality.

These TASO numbers are derived in conjunction with an AM-VSB receiver, and the same are modified in this report to determine FM signal requirements.

For the frequencies considered, the atmospheric attenuation is the most important propagation factor to be discussed. These losses are mainly due to clear weather absorption, cloud and rain attenuation. Hence, they are weather dependent and the attenuation statistics are to be obtained from existing meteorological data, using accepted theoretical or experimental coefficients for converting the various meteorological concentrations into radio attenuation values. This has been done through the use of a suitably designed sampling procedure by involving daily climatological data for one complete year.

Snow, wet snow, hail, fog, etc. also cause attenuation of radio waves. For snow and hail approximate computations may be made given their shape, orientation and a description of their dielectric properties. For others, such as fog, empirical measurements are required. The effects of snow are generally ignored since the attenuation of snow is small compared with that of rain. The same is true of dry sleet and hail. Wet hail and melting snow may be modeled as very large raindrops. However, since little data are available about their effects, they will be ignored.

The performance of any communication system is a function of signal-to-noise ratio, and hence it is important to know the sky noise contribution. This, along with the noise level of the receiver, determines the total noise level of the overall system. Fortunately, the atmospheric noise may be assumed to be proportional to the atmospheric attenuation and this simplifies the statistical analysis of the noise levels.

By means of such a statistical analysis, a method has been developed to determine the picture quality contours for direct television reception from synchronous satellites over a given coverage area.

II. ATTENUATION DUE TO OXYGEN AND WATER VAPOR

Oxygen and water vapor are the two known contributors to the absorption of electro-magnetic waves in atmospheric gases. Even though electrically non-polar, oxygen gas absorbs microwaves because the permanent magnetic dipole moment of the oxygen molecule interacts with the electro-magnetic fields. Water vapor molecules have permanent electric dipole moments that cause microwave absorption. These dipole moments, when excited by an elctro-magnetic wave, oscillate and rotate with many degrees of freedom, each associated with a quantized energy level $h\upsilon$. Thus the molecules absorb discrete amounts of energy from the wave and are raised to a higher energy level; in returning to a lower level they radiate energy isotropically, and therefore the net result is an attenuation of the incident wave.

Oxygen has a band of resonance absorption lines in the region around 5mm. There is another at 2.5 mm. At atmospheric pressure the 5mm lines broaden enough so that they nearly form a single line. Various estimates have been made of a single broadening parameter which can best approximate the observed line shape. Besides this resonant absorption, there is also a continuous non-resonant absorption, at long wavelengths due to diagonal matrix elements.

Water vapor has a weak absorption line near 1.35 cm, and a number of stronger lines below 0.2 cm, the far tails of which contribute to the

7

absorption in the centimeter wavelength region. The shapes of water

vapor resonance curves are dependent on atmospheric temperature, pressure

and partial pressure of water vapor, whereas the shapes of the oxygen

resonance curves are a function of atmospheric temperature and pressure.

A resonance line is generally described by an empirically determined

parameter denoted as the line-breadth constant. The absorption due to

oxygen and water vapor were predicted theoretically by Van Vleck [23,

24] in 1942, and they account most closely for the observed absorption

data.

Three methods for measuring atmospheric attenuation may be cited:

(1) there is the laboratory technique, wherein the attenuation of energy

through a long cylinder, with a controlled amount of water vapor and

oxygen at a given pressure, is measured, (2) attenuation may be measured

by observing the extinction of an extra-terrestrial source as a function

of Zenith angle and (3) atmospheric emission is measured and the corre-

sponding attenuation calculated using an assumed atmospheric mean

temperature.

Van Vleck's formulas for absorption of oxygen and water vapor, as

given by Falcone [25] are as follows:

oxygen absorption coefficient in dB/km

$$= \gamma_0 = \frac{0.358\rho_{0_2}}{T\lambda^2} \left[\frac{(\Delta v)_1}{(\frac{1}{\lambda})^2 + (\Delta v)_1^2} + \frac{(\Delta v)_2}{(\frac{1}{\lambda_0} - \frac{1}{\lambda})^2 + (\Delta v)_2^2} \right.$$

$$\left. + \frac{(\Delta v)_2}{(\frac{1}{\lambda_0} + \frac{1}{\lambda})^2 + (\Delta v)_2^2} \right] \tag{1}$$

where

$(\Delta v)_1$ = line-breadth constant at sea level for the non-resonant part of absorption with dimensions in cm^{-1},

$(\Delta v)_2$ = line-breadth constant for resonant part in cm^{-1}.

λ = wavelength at which absorption is being calculated in cm.

λ_0 = resonant wavelength of oxygen (0.5 cm)

and

$$\rho_{0_2} = 0.385 \times 0.21 \frac{P}{T} \tag{2}$$

where

P = pressure in millibars

T = temperature in $^\circ K$.

Water vapor absorption coefficient, in dB/Km, is given by

$$\gamma_\omega = \frac{\rho_{H_{20}} \times 4.77 \times 10^4 \times 10^{-\frac{278}{T}}}{T^{5/2}\lambda^2} \left[\frac{(\Delta v)_3}{(\frac{1}{\lambda_0} - \frac{1}{\lambda})^2 + (\Delta v)_3^2} \right.$$

$$\left. + \frac{(\Delta v)_3}{(\frac{1}{\lambda_0} + \frac{1}{\lambda})^2 + (\Delta v)_3^2} \right] + \frac{[0.207\rho_{H_{20}}+14.4]\rho_{H_{20}}(\Delta v)_3}{T\lambda^2} \qquad (3)$$

Where

λ_0 = resonant wavelength of water vapor (1.35 cm)

$$(\Delta v)_3 = 1.51 \times 10^{-3} \frac{P}{T^{1/2}}[1 + 3.7 \frac{e}{P}] \qquad (4)$$

e = water vapor pressure in millibars.

$\rho_{H_{20}}$ = water density in g/m^3

Bean and Abbott [26] modified Van Vleck's formula for absorption by oxygen due to the resonance line at 0.5 cm wavelength as follows:

$$\gamma_0 = \frac{0.34}{\lambda^2} \left[\frac{(\Delta v)_1}{(\frac{1}{\lambda})^2 + (\Delta v)_1^2} + \frac{(\Delta v)_2}{[\frac{1}{\lambda} - \frac{1}{0.5}]^2 + (\Delta v)_2^2} + \frac{(\Delta v)_2}{[\frac{1}{\lambda} + \frac{1}{0.5}]^2 + (\Delta v)_2^2} \right]$$

$$(5)$$

Whereas Bean and Dutton [27] describe the water vapor absorption due to the 1.35 cm line at a temperature of 293°K, by

$$\gamma_\omega = \frac{0.0035\rho_{H_2O}}{\lambda^2} \left[\frac{(\Delta v)_3}{[\frac{1}{\lambda} - \frac{1}{1.35}]^2 + (\Delta v)_3^2} + \frac{(\Delta v)_3}{[\frac{1}{\lambda} + \frac{1}{1.35}]^2 + (\Delta v)_3^2} \right. $$
$$\left. + 0.012 (\Delta v)_4 \right] \tag{6}$$

It may be seen from the above that the calculated values of absorption depend on the choice of line-breadth constant (Δv), which represents the effect of broadening by collision. Various investigators have determined the values for (Δv) and they are listed in Table 1.

In the present work, the following values are used for line-breadth constants.

$$(\Delta v)_1 = (\Delta v)_2 = 0.025 \text{ cm}^{-1} \tag{7}$$

$$(\Delta v)_3 = 0.11 \text{ cm}^{-1} \tag{8}$$

and

$$(\Delta v)_4 = 4 \times 0.11 \text{ cm}^{-1} \tag{9}$$

Based on these, the absorption coefficients for oxygen and water vapor are computed for the frequency range 8 to 15 GHz and are plotted as shown in Figure 2. Some of the available measured values are also indicated in the figure.

TABLE 1: CHOICE OF LINE-BREADTH CONSTANTS IN cm^{-1}.

Investigator	Oxygen		Water Vapor	
	$(\Delta v)_1$	$(\Delta v)_2$	$(\Delta v)_3$	$(\Delta v)_4$
Van Vleck [23, 24]	0.02	0.02	0.1	0.1
Becker and Autler [28]	----	----	0.087±0.01	0.087±.01
Bean and Dutton [27]	0.018	0.049	0.087	0.348
Dicke, et.al. [29] (Calculated)	----	----	0.11	0.11
(Measured)			0.12	0.12
Artman and Gordon [30]	0.049	0.049	----	----
Straiton and Tolbert [31]	0.02	0.02	0.1	0.1
Falcone [25]	0.025	0.025	----	----
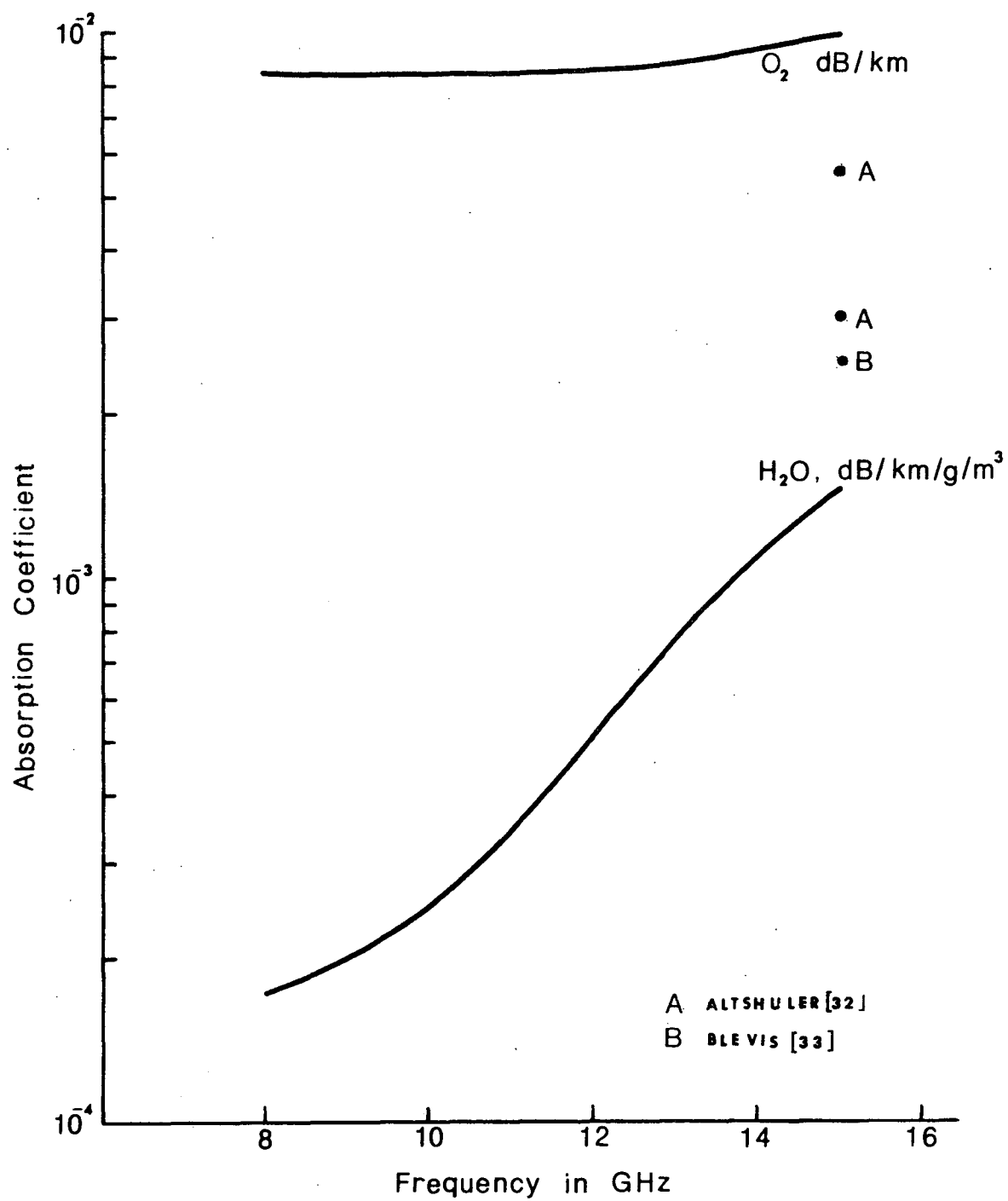
Figure 2. Absorption Coefficients for Oxygen and Water Vapor in the Frequency Range 8-16 GHz.

The National Bureau of Standards has derived an empirical function for the total atmospheric attenuation due to oxygen and water vapor, based on Blake's results [34].

This may be stated as follows:

$$A_g = A_1(f) \cdot A_2(r) \cdot A_3(\theta) \tag{10}$$

Where

A_g = total atmospheric attenuation, in dB.

$$A_1(f) = 1.4 + 0.09f - 1.6 \exp(-2.1f) \tag{11}$$

$$A_2(r) = 1 - \exp(-0.0054r) \tag{12}$$

$$A_3(\theta) = \exp(-10\theta) \qquad \cdot \tag{13}$$

and

f = frequency in GHz

r = length of the raypath in km

θ = elevation angle in radians of the raypath above the horizontal

It may be seen from the above that the attenuation is not dependent on water vapor content in the atmosphere, but only depends on frequency,

path length and elevation angle. Since Blake's results are for frequencies up to 10 GHz, the above empirical formula may be safely used for frequencies up to 10 GHz.

The effects of oxygen and water vapor have been examined so far for a homogeneous medium. These results can be applied to a horizontally stratified atmosphere and used to estimate total atmospheric attenuation as a function of meteorological conditions and location of the satellite terminal. A model of a standard atmosphere is shown in Figure 3. Only the lower 20 km of the atmosphere are shown, since the contributions from oxygen and water vapor above that altitude are negligible at the frequencies of interest here. It may also be noted that the decay constants of oxygen and water vapor decrease with altitude. For example, Bean [35] reports that for a frequency of 10 GHz, both the oxygen and water vapor value at the 7.6 km level is about 17% of that at the ground.

In order to account for the variation of attenuation in the troposphere, an effective vertical path may be assumed. Castelli [36] assumes a path of 11.1 km, whereas Benoit [37] uses a 10 km path. A path of 10 km is assumed in this work to compute the total vertical attenuation. Then the formula for vertical attenuation due to oxygen and water vapor at 12 GHz may be derived as

$$A_{gv} = (0.085 + 5.28 \times 10^{-3}\rho_{H2O})dB. \tag{14}$$
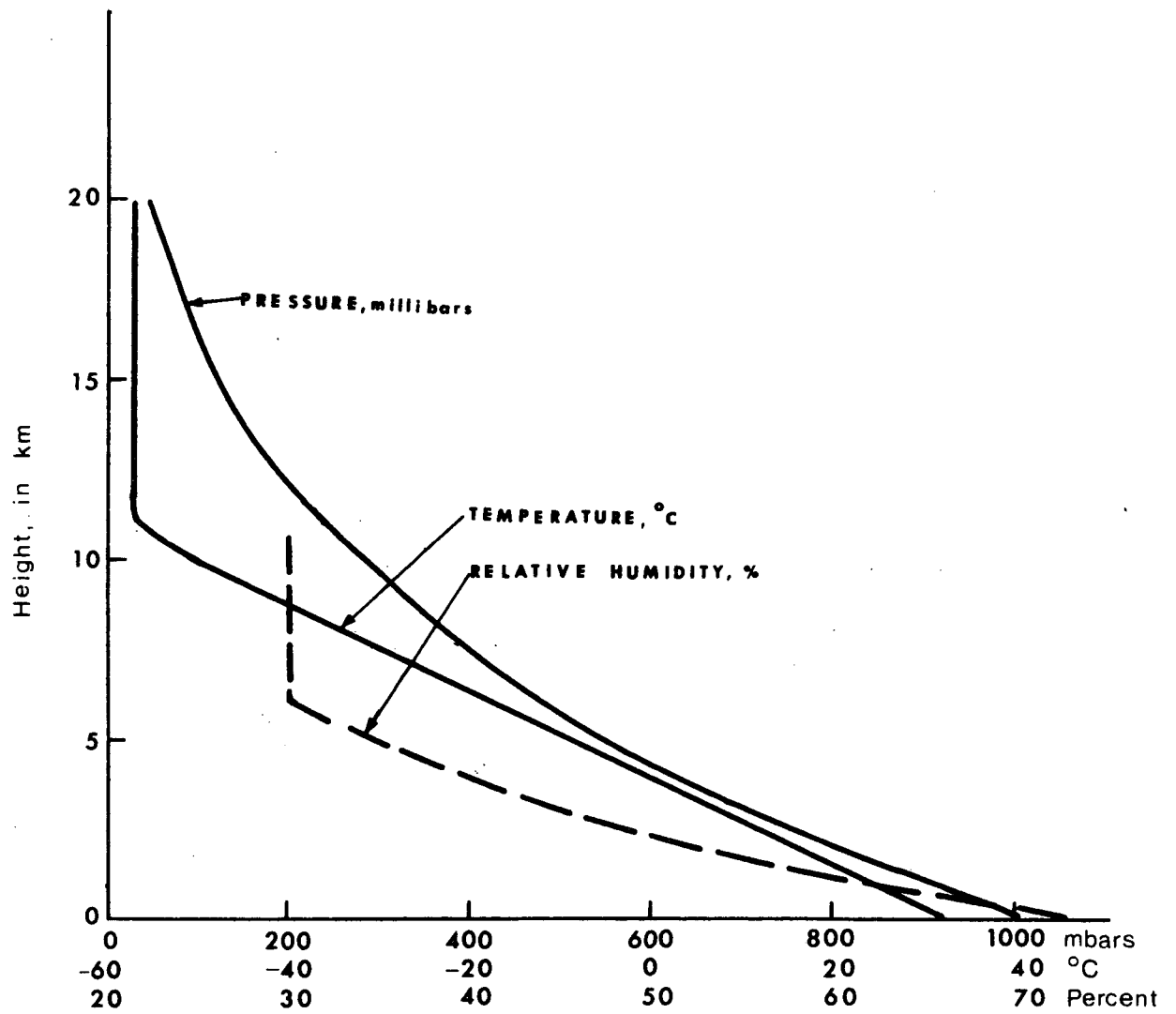
Figure 3. Model of Standard Atmosphere. [32]

For any other elevation, the effective path length is given by

$$r = [r_0^2 \sin^2\theta + r_v(2r_0 + r_v)]^{1/2} - r_0 \sin\theta. \qquad (15)$$

where

r_0 = radius of earth (6371 km)

θ = elevation angle in degrees

r_v = vertical path (10 km)

and attenuation for this path is given by

$$A_g = A_{gv} \frac{r}{r_v} \text{ dB.} \qquad (16)$$

The total Zenith attenuation for the frequency range 8-15 GHz has been computed, as shown in Figure 4. Also shown in this figure are the values used by some other investigators. It may be noted from this figure that the attenuation at 12 GHz used in this work represents a good estimate.
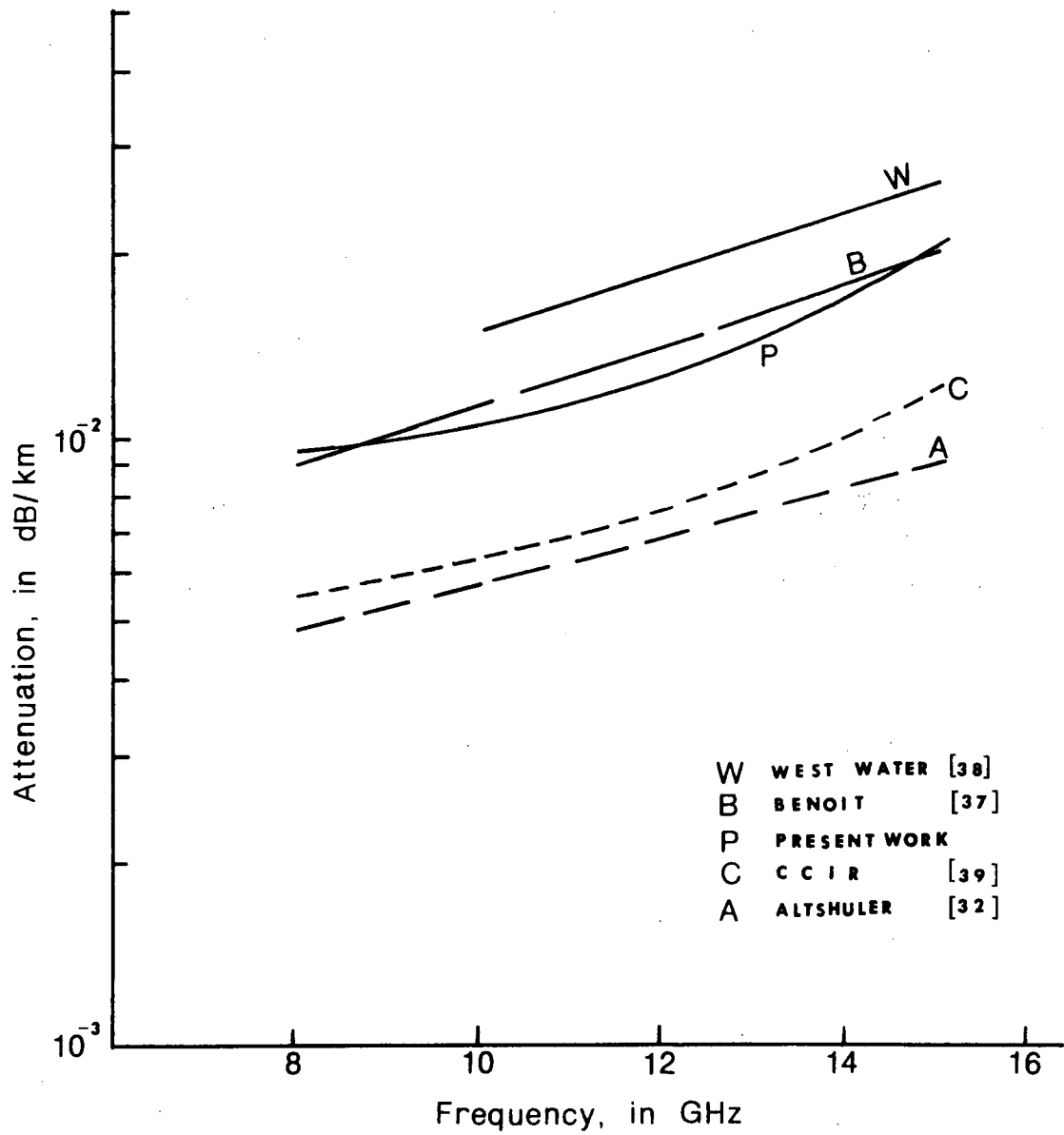
Figure 4. Total Zenith Attenuation due to Oxygen and Watervapor
for Frequency Range 8-15 GHz.

III. ATTENUATION DUE TO CLOUDS AND FOG

As in a gaseous absorption, microwave attenuation due to clouds and fog varies with frequency. The attenuation is due to both absorption and scattering. Cloud droplets are generally less than 100μm in diameter, and since the diameter is much less than the wavelength (2.5 cm), Rayleigh approximation holds, and the losses may be considered mainly due to absorption rather than scattering. Temperature and dielectric constant of the droplets also contribute. Attenuation increases as the temperature of water in clouds decreases until the transition from water to ice is passed, at which point a new dielectric constant takes effect and the attenuation becomes considerably less. It has been shown that attenuation depends more on total liquid water content than on droplet-size distribution.

The attenuation by clouds of a signal transmitted towards the earth can be evaluated on the basis of the data presented by Gunn and East [40], through the simplified global formula

$$A_c = k_c \rho_c R \tag{17}$$

where A_c = Attenuation due to cloud in dB.

k_c = Coefficient of attenuation for clouds in dB/km/g/m^3

ρ_c = Water content of clouds in g/m^3

R = Signal path through the cloud in km

Benoit [37] has expressed the coefficient k_c in terms of frequency,

type of clouds, (water or ice) and on temperature by the following relationships.

$$k_{cw} = f^{b_w} \cdot \quad \exp[a_{ow} (1 + mt)] \tag{18}$$

and

$$k_{ci} = f^{b_i} \cdot \quad \exp[a_{oi} (At^2 + Bt + 1)] \tag{19}$$

where

k_{cw} = Coefficient for water cloud

k_{ci} = Coefficient for ice cloud

f   = Frequency in GHZ

t   = Temperature in ° C.

and a_{ow}, b_w, a_{oi}, b_i, m, A and B are constants as listed in Table 2.

TABLE 2:   CONSTANTS USED IN RELATIONSHIPS OF
ATTENUATION COEFFICIENT FOR CLOUDS.

Water Clouds	Ice Clouds
a_{ow} = -6.866 b_w = 1.95 m = 4.5 X 10^{-3}	a_{oi} = -8.261 b_i = 1.006 A = -4.374 X 10^{-4} B = -1.767 X 10^{-2}

Using the above relationships, coefficient k_c has been computed for the frequency range 8 - 16 GHZ and is shown in Figure 5 for different cloud conditions. The values of Gunn and East are indicated and the curves computed by Bean [35] and Mitchell [41] are compared. The results
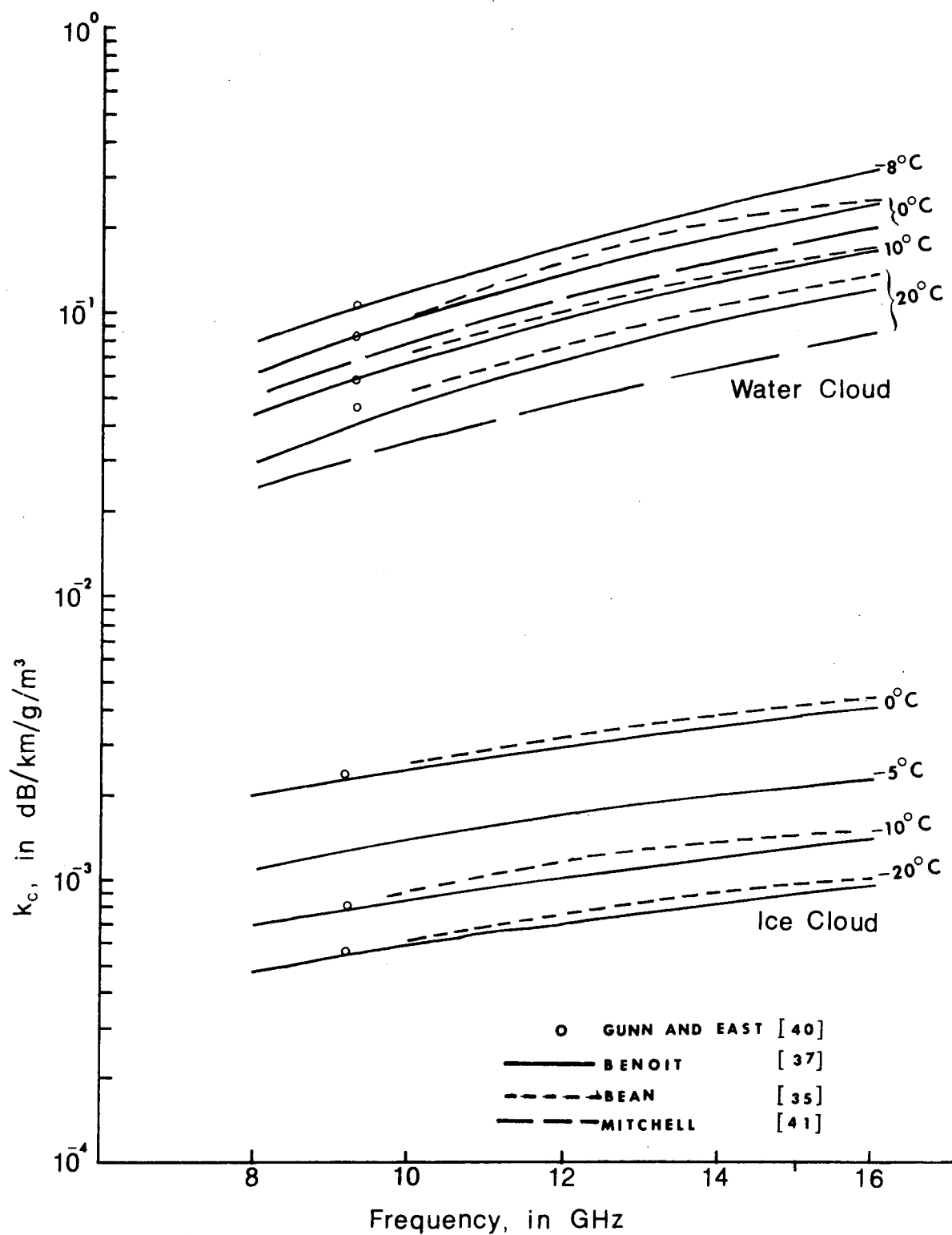
Figure 5.   Attenuation Coefficient for Clouds for Frequency Range
8-16 GHz and for Various Temperatures.

show good agreement.

The water content of a cloud may range anywhere from a small fraction to 3 or 4 g/m^3. A model of atmosphere with precipitation for temperate regions is shown in Figure 6. The horizontal extent of the cloud can be several hundred km in any direction, although its vertical thickness rarely exceeds 6 km. Hence the signal path length R may be taken as $(\frac{6}{Sin\theta})$ where θ is the elevation angle in degrees.

Fog is caused by water droplets suspended in the air in sufficient concentrations to reduce the visibility at the ground below 1000 meters. The attenuation due to fog varies with frequency, temperature and visibility. The decay constant of fog, as calculated by Ryde [42], is plotted in Figure 7, along with the results of Erwin Mondre [43].

It may be seen that the attenuation at 20°C is about a factor of one-half smaller than at 0°C for a given visibility.

Signal loss in snow is the result of both scattering and absorption. Atlas et al. [44] have shown that snow exhibits very small attenuation at x-band frequencies.
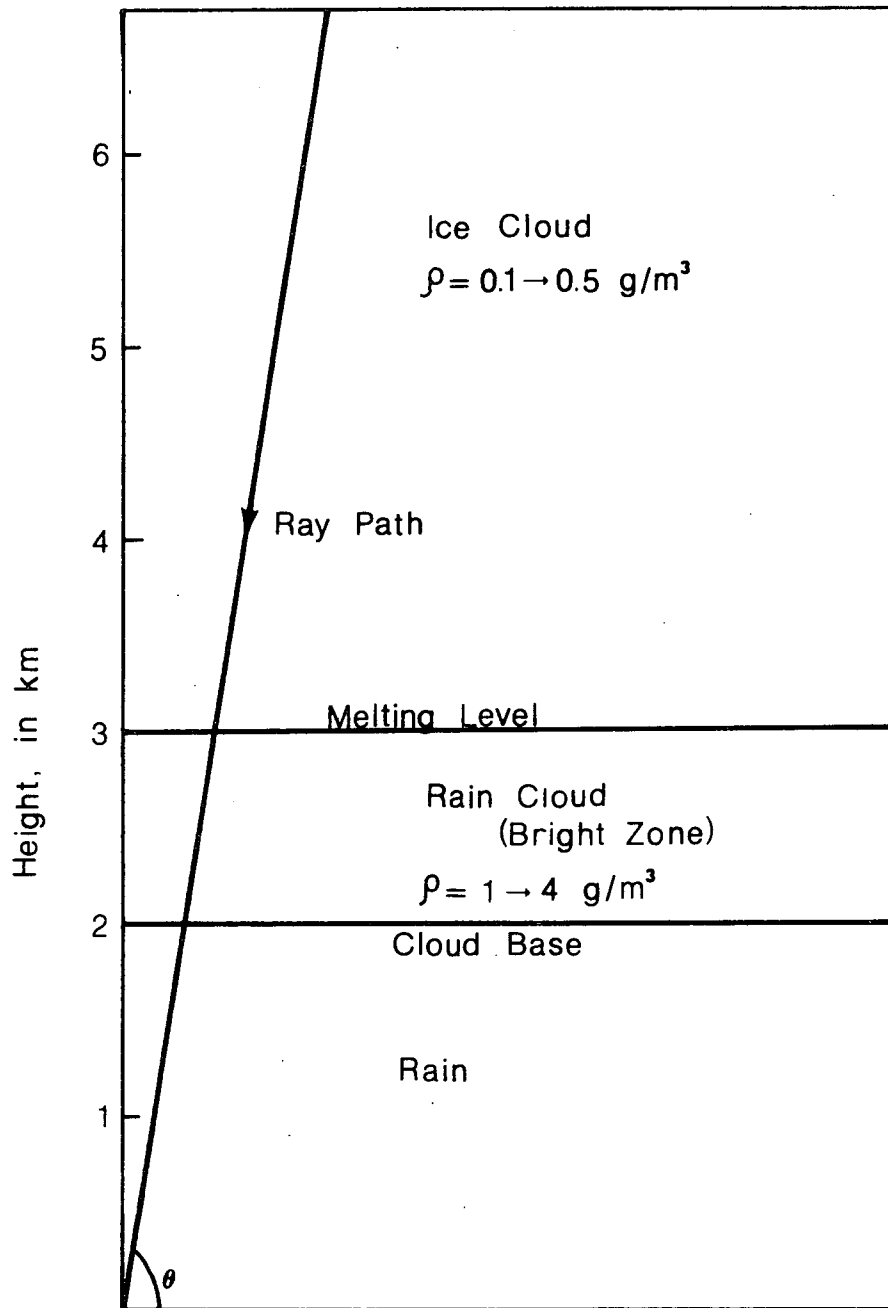
Figure 6. Model of Atmosphere with Precipitation for
Temperate Regions. [32]
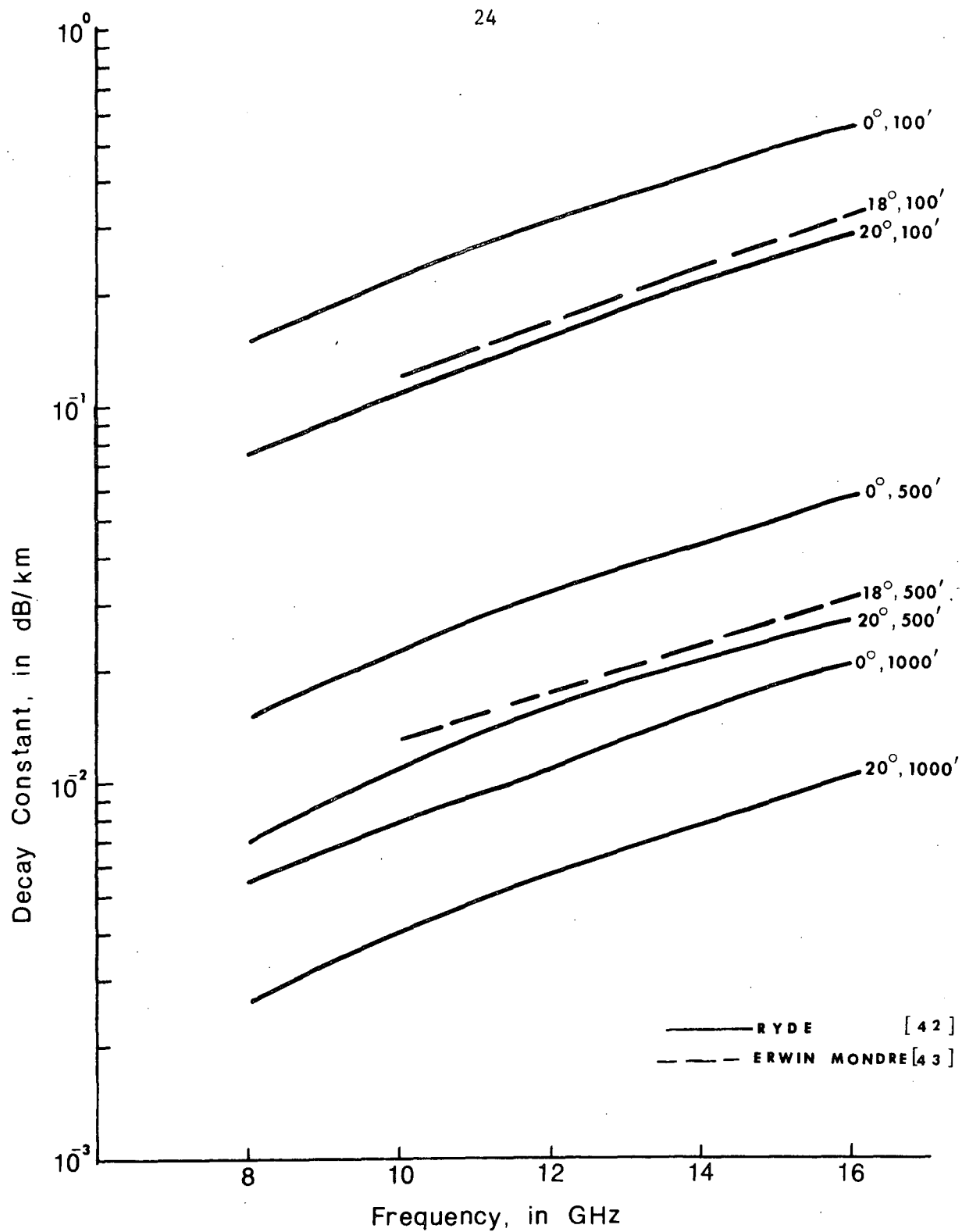
Figure 7. Decay Constant of Fog for Frequency Range 8-16 GHz and
at Various Temperatures and Visibility.

IV. ATTENUATION DUE TO RAIN

Precipitation in the form of rainfall is the largest factor in atmospheric attenuation in the temperate regions of the world. The sizes of water drops and the distribution of these sizes along the propagation path are the controlling factors. Since the absorption and scattering coefficients of water drops is well established, the attenuation due to a homogenous rain of a given rate can be computed. The attenuation increases rapidly with drop size, which increases with rainfall rate and frequency.

The theory of scattering by a single lossy dielectric sphere is based upon a series solution to the scattering problem and was first given by Mie [45] in 1908. Stratton [46] has derived the same by considering the interaction of a plane wave-front with a single spherical drop. The analysis by Ryde [47, 48, 49] results in the following for a hypothetical rain consisting of drops of equal diameter and uniform drop concentration.

$$\text{Attenuation} = A = 0.4343 \frac{N\lambda^2}{2\pi} A_i \times 10^6 \text{ dB/km} \qquad (20)$$

where

N = Number of drops per cubic centimeter.

λ = Wavelength in cm.

$$A_i = \text{Real part of } \sum_{n=1}^{\infty} (a_n + b_n) \qquad (21)$$

$$a_n = (2n + 1) \left[\frac{j_n(\alpha)[m\alpha j_n(m\alpha)]' - j_n(m\alpha)[\alpha j_n(\alpha)]'}{j_n(m\alpha)[\alpha h_n^{(1)}(\alpha)]' - h_n^{(1)}(\alpha)[m\alpha j_n(m\alpha)]'} \right] \tag{22}$$

$$b_n = (2n + 1) \left[\frac{m^2 j_n(m\alpha)[\alpha j_n(\alpha)]' - j_n(\alpha)[m\alpha j_n(m\alpha)]'}{h_n^{(1)}(\alpha)[m\alpha j_n(m\alpha)]' - m^2 j_n(m\alpha)[\alpha h_n^{(1)}(\alpha)]'} \right] \tag{23}$$

$$j_n(x) = \sqrt{\frac{\pi}{2x}} \, J_{(n+\frac{1}{2})}(x) \tag{24}$$

$$\eta_n(x) = \sqrt{\frac{\pi}{2x}} \, J_{-(n+\frac{1}{2})}(x) \left\{ (-1)^{n+1} \right\} \tag{25}$$

$J_v(x)$ = the Bessel function of the first kind of order v.

$$h_n^{(1)}(x) = j_n(x) + i\eta_n(x) \tag{26}$$

$$\alpha = \frac{\pi D}{\lambda} \tag{27}$$

D = Drop diameter in cm.

λ = Wavelength in cm.

$m = m_1 - im_2$ = square root of the complex dielectric $\qquad$ (28)

constant of water.

The following assumptions are made in the above formula.

(1) Rain drops are spherical.

(2) Dielectric constant of water in the drops is uniform and known.

(3) Single scattering theory is sufficient to evaluate scattering

from a volume of rain drops.

(4) The drops are randomly scattered, with uniform average density,

throughout the space of the ray path.

(5) The assumption of a plane wave-front at each drop position is

adequate, and

(6) the interaction between drops is negligible.

Using these assumptions, the attenuation coefficient is determined

from the imaginary part of the effective index of refraction of the

medium and is proportional to the sum of the total scattering and

absorption cross section per unit volume averaged over the drop size

distributions applicable to the unit volume. The attenuation

coefficient thus obtained describes the behavior of the expected value

of the amplitude of the wave propagating through the medium or the

so called 'coherent' signal propagating through the medium.

The fundamental physical quantity in the above expression is m.

Medhurst [50] uses the semi-empirical expressions given by Saxton [51].

They are

$$m_1 = \frac{1}{\sqrt{2}} \left[\sqrt{\frac{\varepsilon_s^2 + \varepsilon_o^2 x^2}{1 + x^2}} + \frac{\varepsilon_s + \varepsilon_o x^2}{1 + x^2} \right]^{1/2} \tag{29}$$

$$\text{and } m_2 = \frac{1}{\sqrt{2}} \left[\sqrt{\frac{\varepsilon_s^2 + \varepsilon_o^2 x^2}{1 + x^2}} - \frac{\varepsilon_s + \varepsilon_o x^2}{1 + x^2} \right]^{1/2} \tag{30}$$

$$\text{where} \quad x = \omega \tau_o = \frac{2\pi \text{ X } 3 \text{ X } 10^{10}}{\lambda} \tau_o \tag{31}$$

ε_s and τ_o are temperature dependent and at 20°C, the values as given by Saxton are

$$\varepsilon_s = 80.08 \tag{32}$$

$$\tau_o = 8.1 \text{ X } 10^{-12} \tag{33}$$

$$\text{and} \quad \varepsilon_o = 5.5 \tag{34}$$

Using these values, the value of m at 12 GHz becomes,

$$m = (8.007 - i2.0716) \tag{35}$$

Further one may define the cross section Q_t of the water drop as the ratio of the total absorbed and scattered energy per second to the energy density of the incident wave and is given by

$$Q_t = \frac{\lambda^2}{2\pi} A_i \qquad cm^2 \quad . \tag{36}$$

Then the attenuation for a given drop spectrum is

$$A = 0.4343 \sum (n(D) Q_t(D) \text{ x } 10^6) \tag{37}$$

In order to relate the attenuation to the precipitation rate

pmm/hr, it is necessary to know the raindrop spectra, i.e. the number

of drops having a given diameter (per cubic meter) for a given rate

of rainfall. Practically, this distribution will vary accoring to wind,

temperature and other conditions. Representative distributions have

been obtained by Laws and Parsons [52], Marshall and Palmer [53], Kelkar

[54], and others. The raindrops are classified in about 15 ranges

of dimension. For each range of diameter D_1, D_2, $\cdots$, D_{15} it is

possible to calculate the attenuation cross section $Q_t(D_1)$, $Q_t(D_2)$ $\cdots$

$Q_t(D_{15})$ and knowing the number of drops $n(D_1)$, $n(D_2)\cdots n(D_{15})$,

attenuation can be expressed by

$$A = 0.4343[n(D_1)Q_t(D_1) + n(D_2)Q_t(D_2) + \cdots + n(D_{15})Q_t(D_{15})] \times 10^6$$

$$(38)$$

The drop distribution may be obtained by one of the following

two methods.

The first method is due to Laws and Parsons. They give represen-

tative drop size distributions in percent of total volume for a given

precipitation. The terminal velocity of rain drops (v m/s) as a

function of drop diameter is given in Figure 1 of Medhurst. Now suppose

that for a particular precipitation rate, say pmm/hr, p_{D_i} is the

proportion of total volume of water reaching the ground which consists

of drops whose diameters fall in the interval centered on D_i cm. Then

it can be shown that

$$n(D_i) = \frac{P_{D_i}}{1.885 \times 10^6 \times v \times D^3} \qquad (39)$$

where $n(D_i)$ = number of drops of diameter D_i cm.

The second method is due to Marshall and Palmer. They fit the experimental observations by an exponential distribution function,

$$N(D) = N_D \exp[-\Lambda D]$$

and $n(D_i) = \displaystyle\int_{(D_i - \frac{dD}{2})}^{(D_i + \frac{dD}{2})} N(D)\, dD$ = number of drops of diameter between

$(D_i - \frac{dD}{2})$ and $(D_i + \frac{dD}{2})$ in unit volume of space $\qquad (40)$

N_o = value of N_D for $D = 0$, which is = 0.08 cm^{-4} and

$$\Lambda = 41\ p^{-0.21}\ cm^{-1}. \qquad (41)$$

This distribution function as compared with the results of Laws and Parsons, and Marshall and Palmer, is shown in Figure 8.

Based on the above, the first comprehensive tabulation of the attenuation coefficient versus rain rate for a large number of frequencies was made by Ryde and Ryde [44,45]. Medhurst [46] corrected and extended this earlier work and compared the updated attenuation curves with the experimental data then available in the literature. He observed
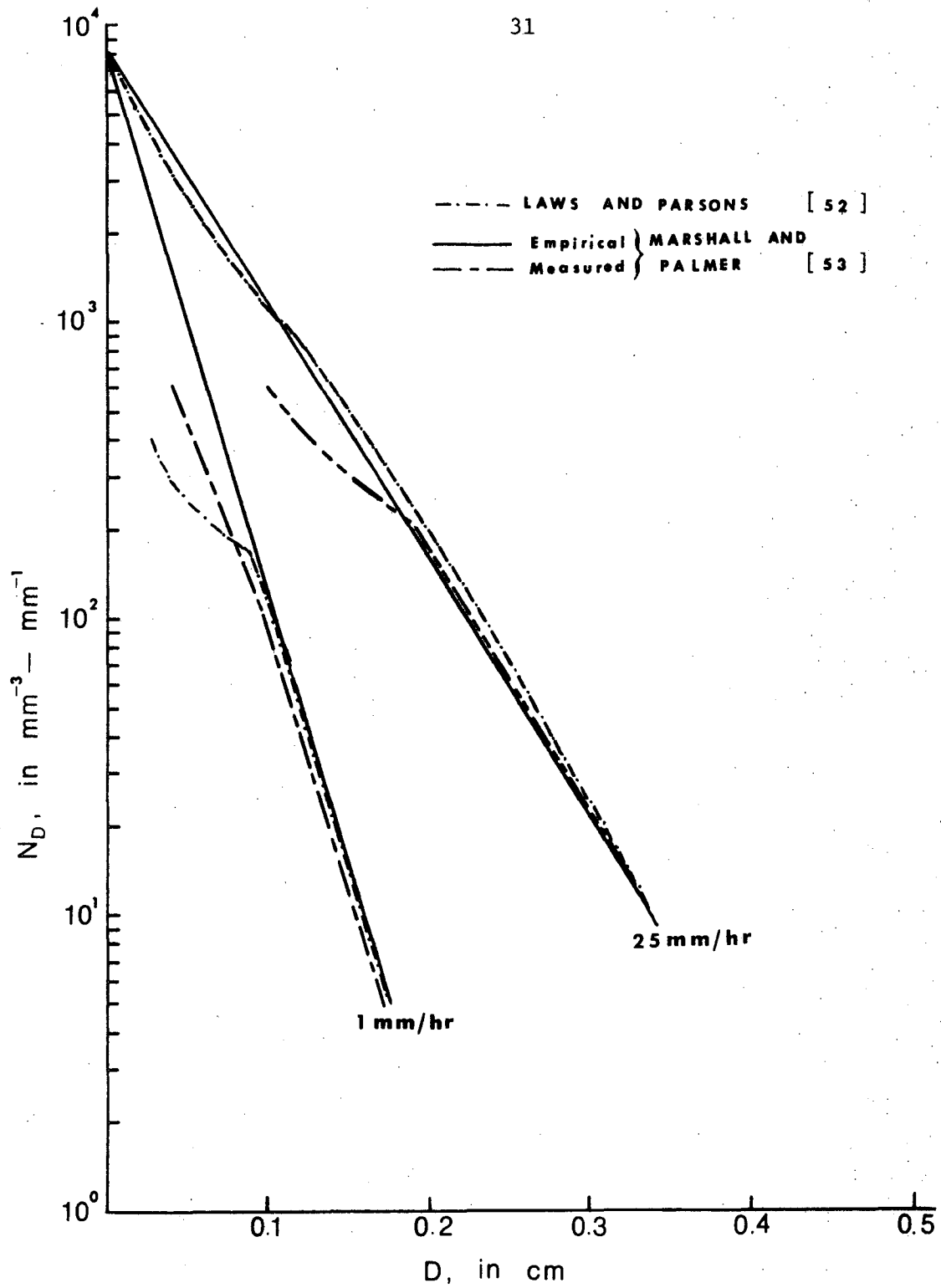
Figure 8. Distribution of Raindrops with Size.

"a marked tendency for the observed attenuations to fall well above the levels which according to the theory, cannot be exceeded." From this he concluded that "the applicability of Mie theory to the practical rainfall situation cannot be said to be demonstrated," and concludes that the attenuation curves obtained by applying the Mie theory to the Laws and Parsons drop size distribution can only be taken as giving a rather crude order of magnitude. The exponential distribution model of Marshall and Palmer consists of more small drops than given in the Laws and Parsons distribution, but otherwise similar to it. Crane [55] has estimated attenuation coefficient versus frequency for both models. It may be seen from his figure (7) that both models would result in almost identical coefficients at least up to 35 GHz. This means that the smaller rain drops have significant effect on attenuation only at frequencies above 35 GHz.

Since the publication of Medhurst's paper, several additional experiments have been performed and almost all of these reported the same tendencies as Medhurst noted. The discrepancy between the measured and predicted attenuation values may be attributed partly to the theory and partly to experimental error, which is due to inadequate handling of meteorological data.

In the theoretical approach, one possible error is the neglect of multiple scattering effects along the path. Wulfsberg and Altshuler [56] have shown that the effect of scattering on measurement accuracy is considered negligible at 15 GHz and significant only at high rain

rates at 35 GHz. (It may be noted that we are interested in frequencies below 35 GHz in this discussion).

Another possible source of error is that the rain structure may be more complex than has been assumed. It has been found that the drop size distributions are not homogenous in space or time. The drop size distribution measured at the surface by a small device may be different from the average drop size distribution present in the actual beam which is large compared to the capture surface of the drop size measuring device.

It may be suspected that both the models of raindrop size spectra used in the above discussions are not satisfactory. This becomes clear if we look at the computations made by Godard [57] using Kelkar's distribution. Comparisons at wavelengths of 10 cm, 5.5 cm and 0.86 cm are made in Figure 9, showing computations of Medhurst and Godard. Two observations may be made from this comparison.

(1) At wavelengths of 10 cm and 5.5 cm, the results of Godard are significantly larger than those of Medhurst, for all rates of rainfall. This means Godard's results are closer to the measured values, than those of Medhurst. This may indicate that the Kelkar's distribution may be more appropriate than either of the earlier two models used.

(2) At 0.86 cm wavelength, there is no significant difference between the two results. This may suggest that with smaller and smaller wavelengths, the effects of variation in raindrop spectra become less and less significant.
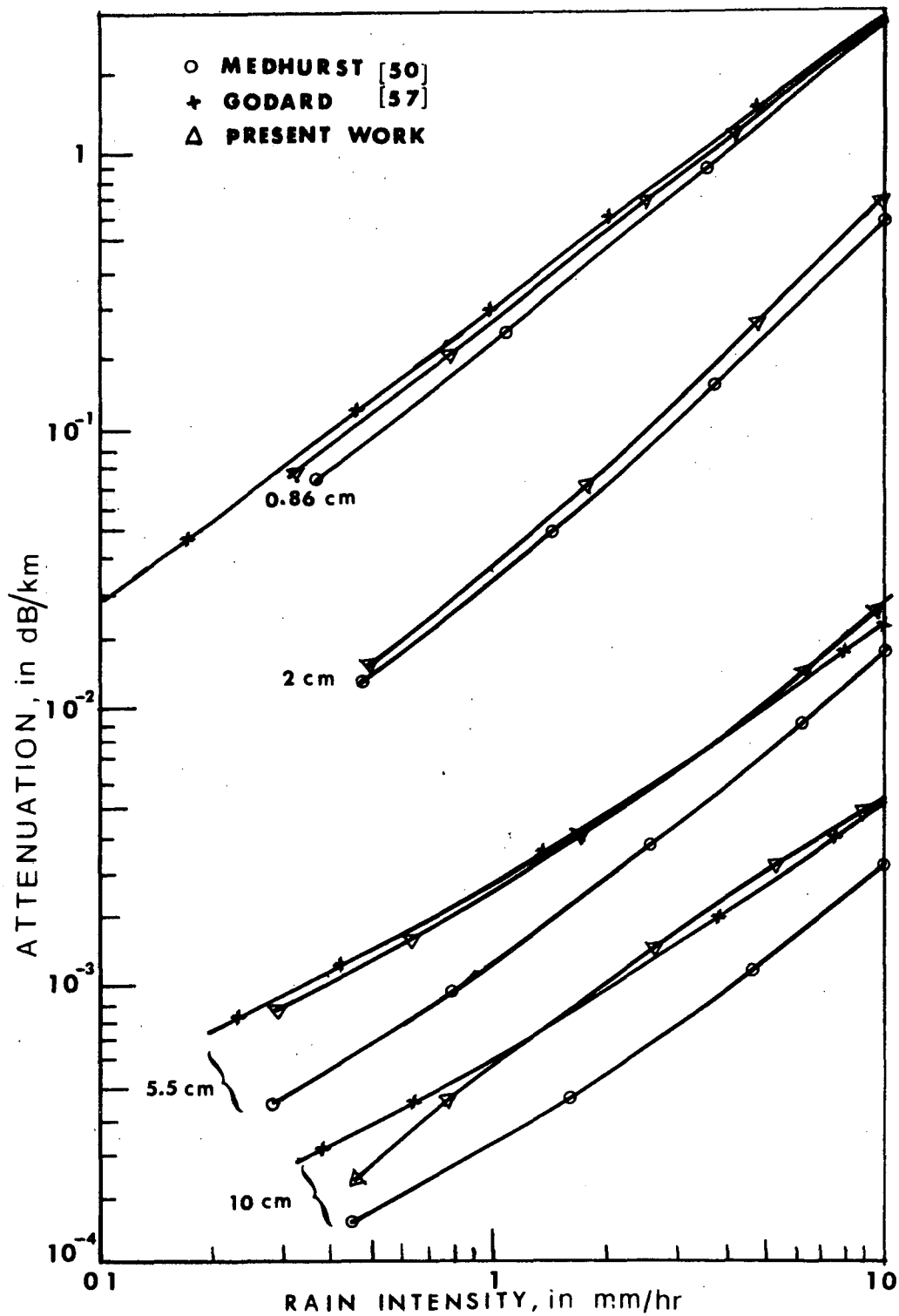
Figure 9. Theoretical Attenuation Versus Rate of Rainfall at
Several Wavelengths.

The second observation gave clue to the possibility of using a new model in the present work for the computation of rain attenuation and the same is explained below.

In the new model, the concept of median diameter is utilized to replace the rain drop spectra for a given rainfall. The median drop diameter is the raindrop diameter dividing the drops of larger and smaller diameter into groups of equal volume. Laws and Parsons have derived the following relation between the median diameter and rate of rainfall.

$$D_{50} = 2.23 \; R^{0.182} \tag{42}$$

where

D_{50} = median diameter in mm.

and

R = rain fall-rate in inches/hr.

Greer [58] has modified the above relationship to the form

$$D_{50} = (2.54 + 0.97 \; \log R) \tag{43}$$

These relations are shown in Figure 10. Since the results of Greer give better results, they are used in the following computations.

In order to calculate the attenuation at a given frequency, for a given rain fall the following steps are taken.

(1) For a given rainfall, the median diameter is computed from equation (43).
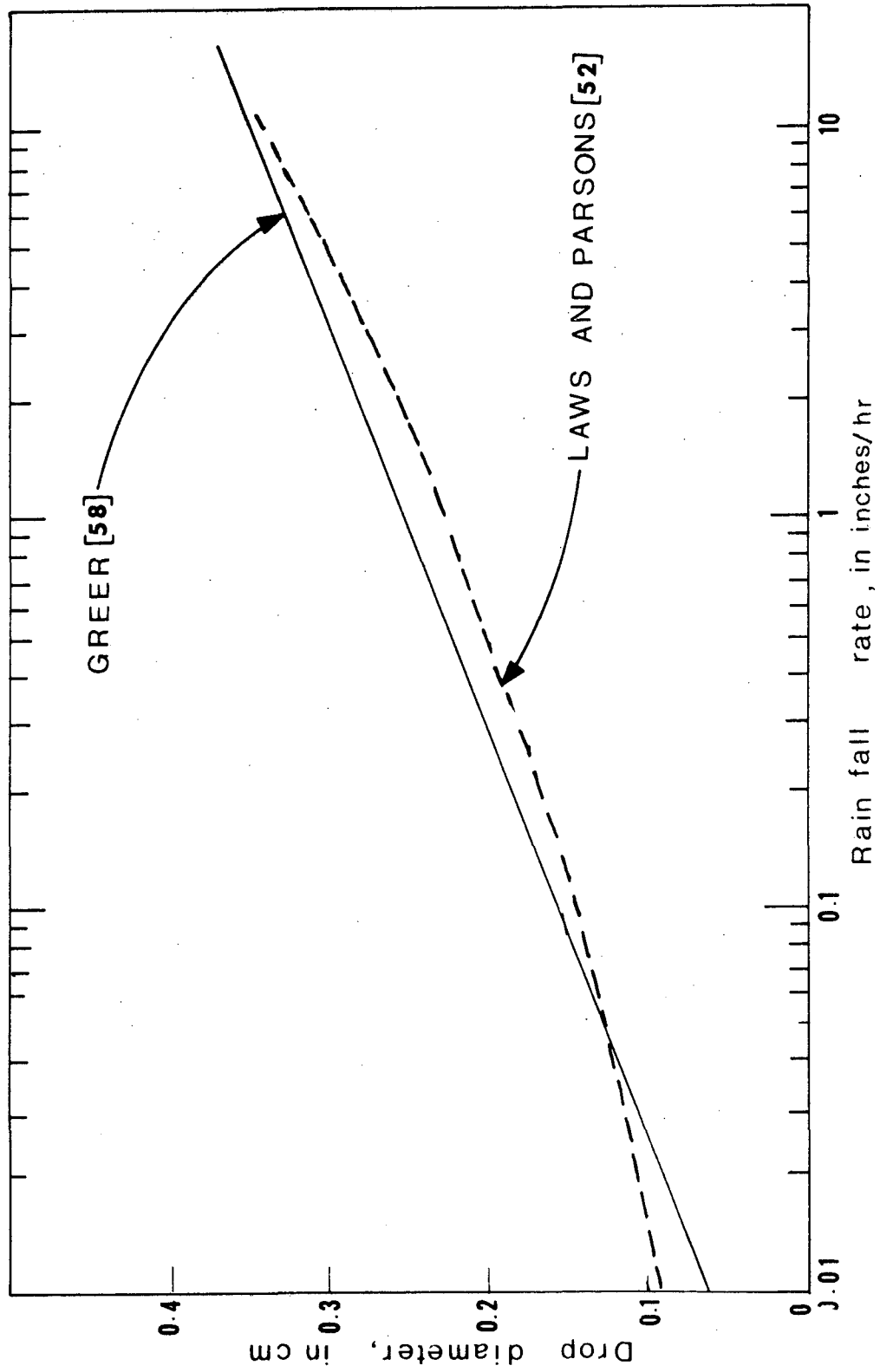
Figure 10. Relationship of Median Raindrop Diameter to Rainfall Intensity.

(2) For this diameter and given λ, Q_t is determined from (36).

(3) It is assumed that the rain consists of only drops of diameter D_{50} and the number of such drops is given by,

$$N_D = \frac{p}{1.885 \times 10^6 \times v \, D_{50}^3} \qquad (44)$$

where p = rainfall rate in mm/hr

v = terminal velocity of raindrop of diameter D_{50}.

The value of v is read from Figure 1 of reference [50], and N_D is calculated.

(4) The attenuation is then given by,

$$A = (0.4343 \, N_D Q_t \times 10^6) \text{ dB/km.} \qquad (45)$$

Computations of attenuation are made for wavelengths of 10 cm, 5.5 cm, 2 cm and 0.86 cm, and for rainfall rates up to 10 mm/hr and the results are plotted in Figure 9. It may be seen that the results of the new model fit almost exactly with the results of Godard. This is true especially at longer wavelengths, where the drop size distribution assumed has a significant effect. In all cases, however, the new model results in higher values of attenuation as compared with those of Medhurst and are therefore closer to the measured values as is shown below. Even though the new model gives good results, no attempts are made to explain the physical phenomena involved with the relation-ship between median diameter and actual rain drop distribution as far as the absorption of microwave energy is concerned.

In the following figures, comparisons are made with some of the measured values. Figure 11 indicates measurements of Robertson and King [59] at $\lambda = 3.2$ cm compared with the analytical results of Medhurst and present computation. Even though slightly better fit is obtained than that of Medhurst, there is still wide dispersion. Of course, this may be attributed to inadequate use of rainfall data, since only one rain gauge was used and no averaging techniques were employed.

Several investigators use an empirical relationship given by Gunn and East [40], of the form $A = k_p p^{\alpha}$. Where k_p and α are frequency dependent parameters. These parameters, as derived by various workers are given in Figures 12 and 13. Figure 14 gives the measurements at 15 GHz, for a path length of 15.78 km by Blevis et al. [55]. Also shown is their empirical formula used, which compares with the theoretical computations based on Laws and Parsons distribution. It may be seen again, that the results of the present model give a better fit for the measured values.

The most encouraging application of the new model seems to be for the earth to Space Communication link. The results based on median diameter used in conjunction with space averaged rainfall rate seem to indicate a good correlation with the measured values as discussed below. It may be that the median drop is a good representation for an earth to space path, since there probably are differences between water drop speeds and distributions near the ground surface and near the cloud.
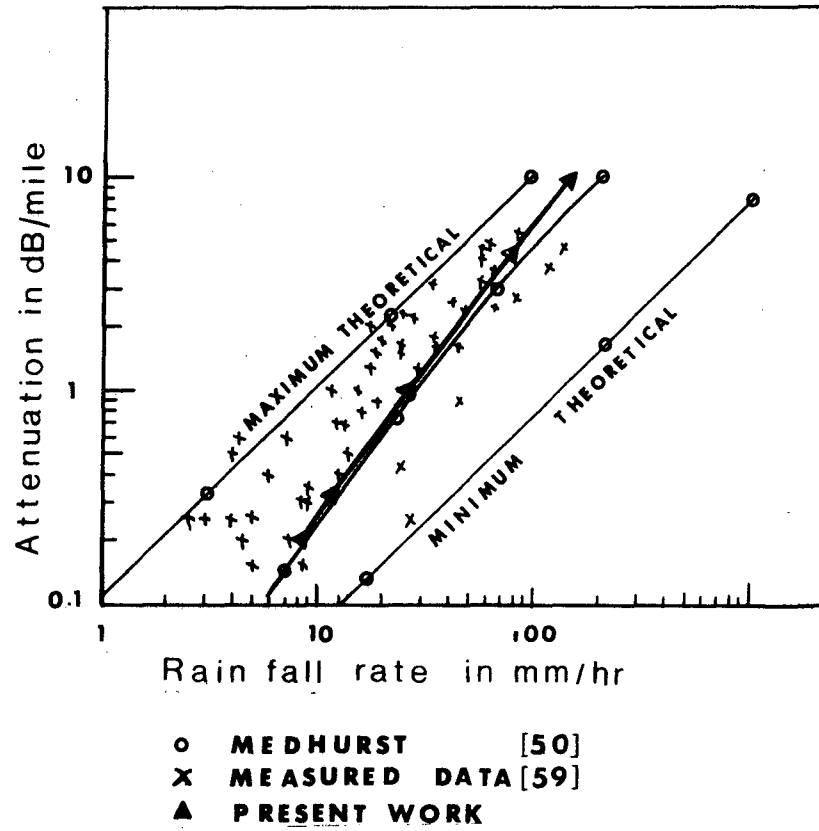
Figure 11. Comparison of Theoretical and Measured Rain Attenuation at 3.2 cm Wavelength. (Measurements by Robertson and King. [59])
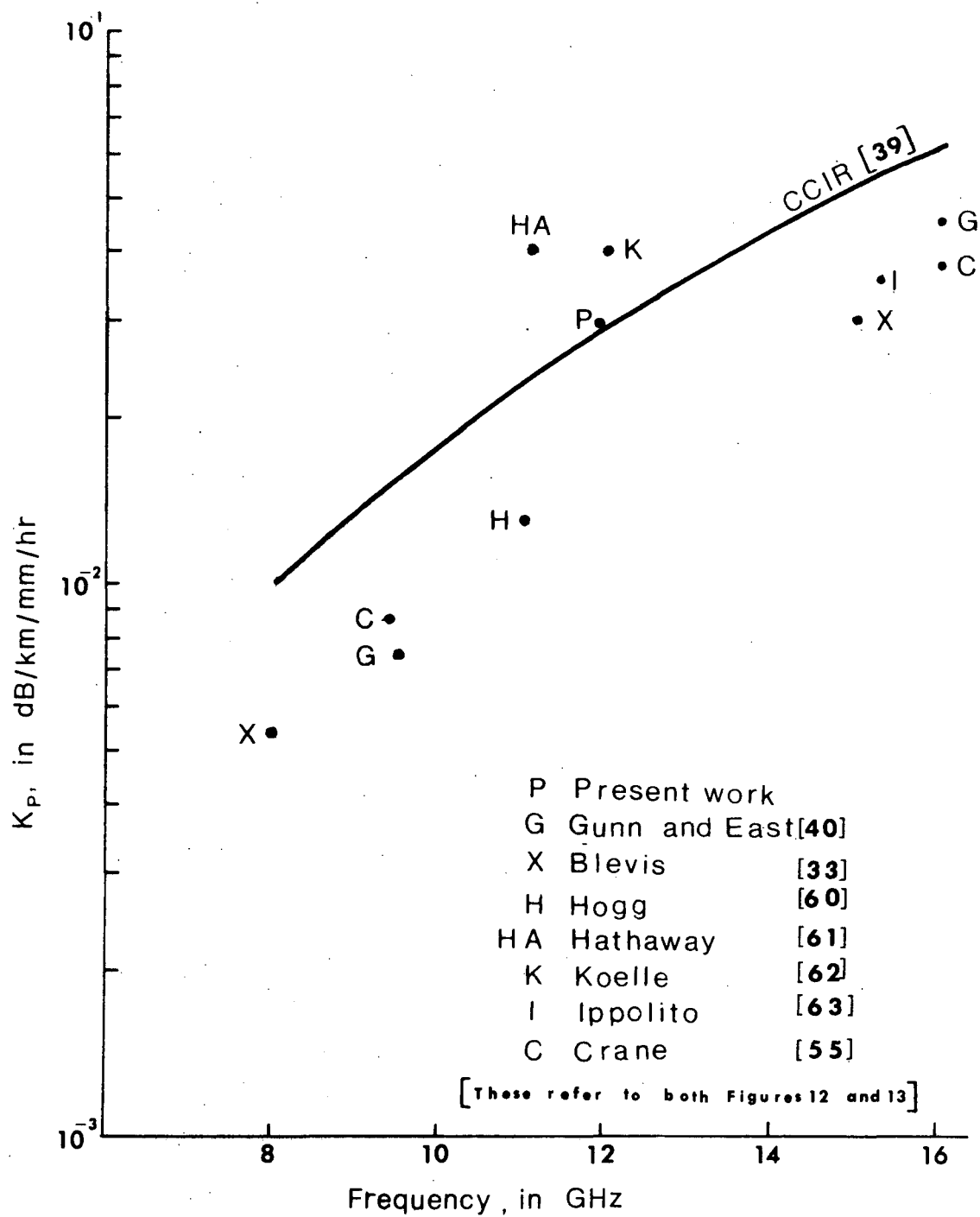
Figure 12.   Coefficient K_p of Rain Attenuation Versus Frequency.
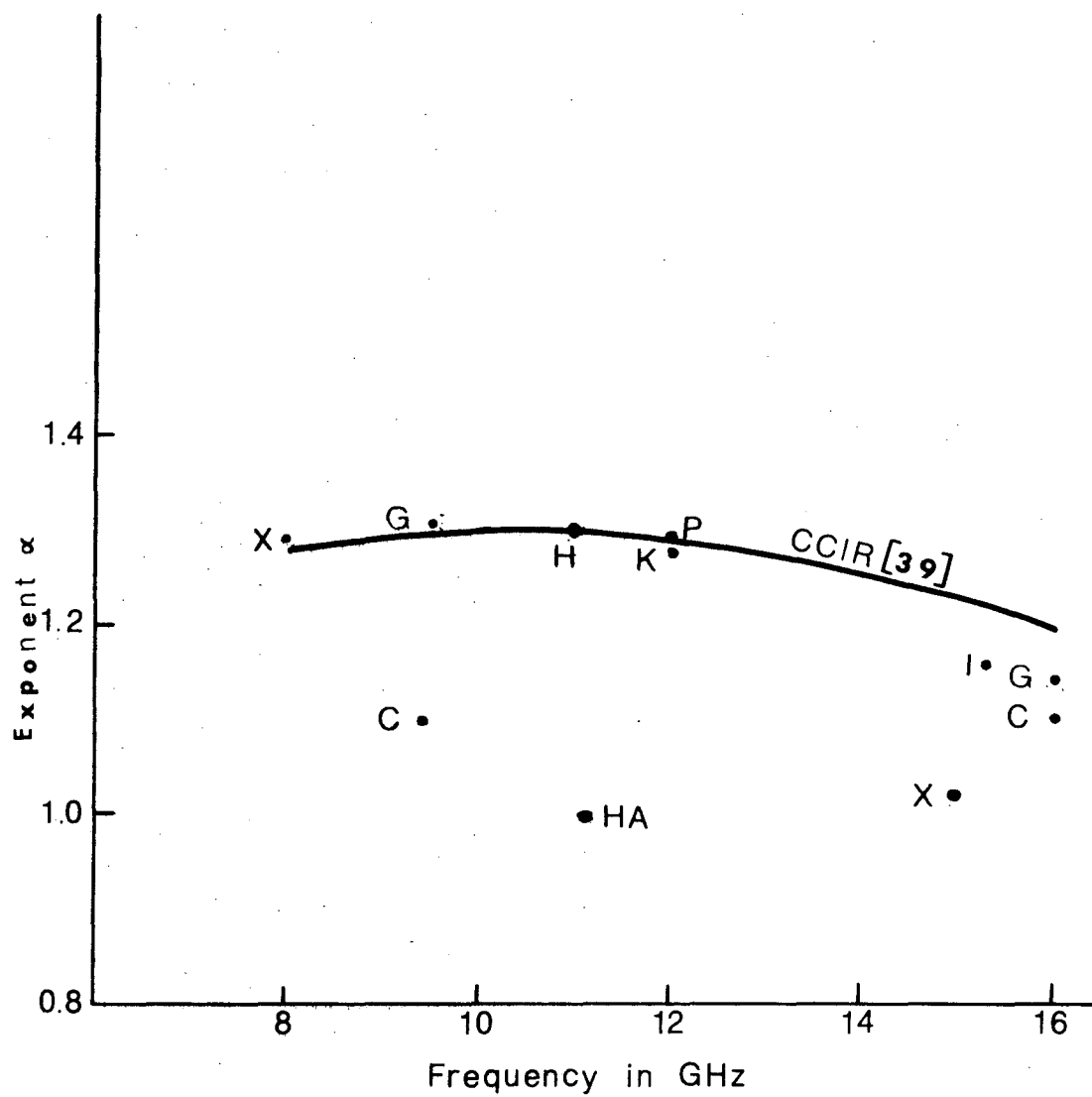
Figure 13. Exponent α of Rain Attenuation Versus Frequency.
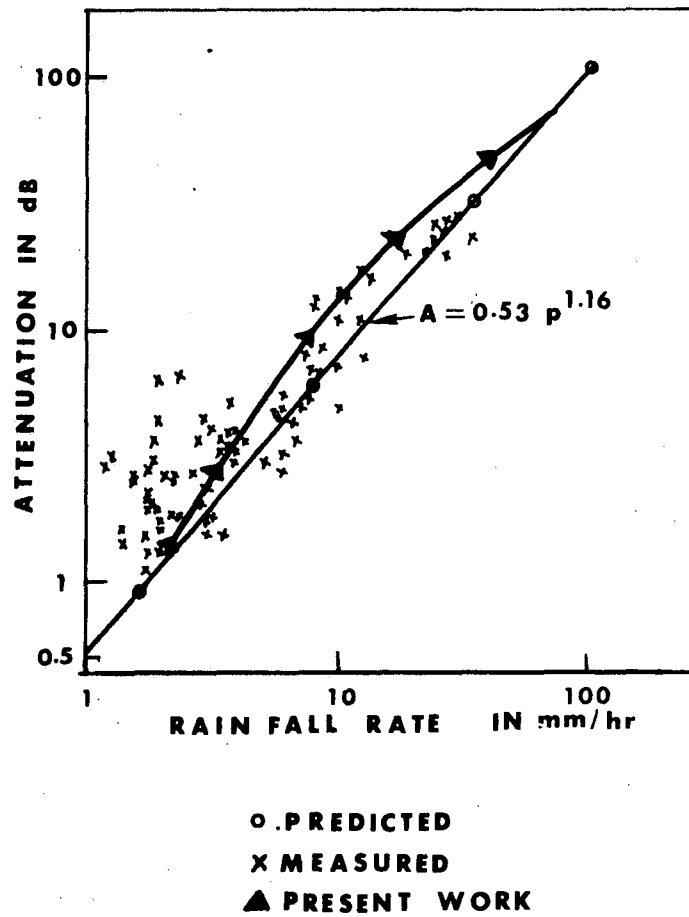
Figure 14. Comparison of Theoretical and Measured Attenuation at
15 GHz for a 15.78 km Path Length. (Measurements by
Blevis, et.al. [33])

Figure 15 is a scatter diagram carrier attenuation at 15.3 GHz versus rainfall rate measured by ATS-V satellite experiment as given by Ippolito [56]. The predicted empirical formula in this case also is based on the earlier two models of raindrop spectra, and the new model results in better agreement with the measured values. However, more definite comments are not made in this case since the precipitation statistics were taken only from two rain gauges placed about 50 meters apart directly in front of the antenna system. The necessity of better averaging techniques is evident from the later results of ATS-V as given by Ippolito [64].

Figures 16 (a), (b) and (c) are taken from Ippolito [64]. The abscissa indicate "near rainfall rate" in (a), "ground averaged rainfall rate" in (b) and "height averaged rainfall rate in (c). Ten rain gauges were used for this measurement and were placed as shown in Figure 17.

The "near rainfall rate" is the rate as given by the nearest gauge located directly in front of the antenna. The "ground averaged rainfall rate" is $\overline{R}(0) = \sum_{n=1}^{10} \frac{R_n(0)}{10}$ where $R_n(0)$ is the reading of

$$(46)$$

the nth bucket. The height average rainfall rate is,

$$\overline{R}(h) = \frac{1}{10} \sum_{n=1}^{10} (1 - \frac{h_n}{H}) R_n(0). \tag{47}$$

where h_n and H are as shown in Figure 17.
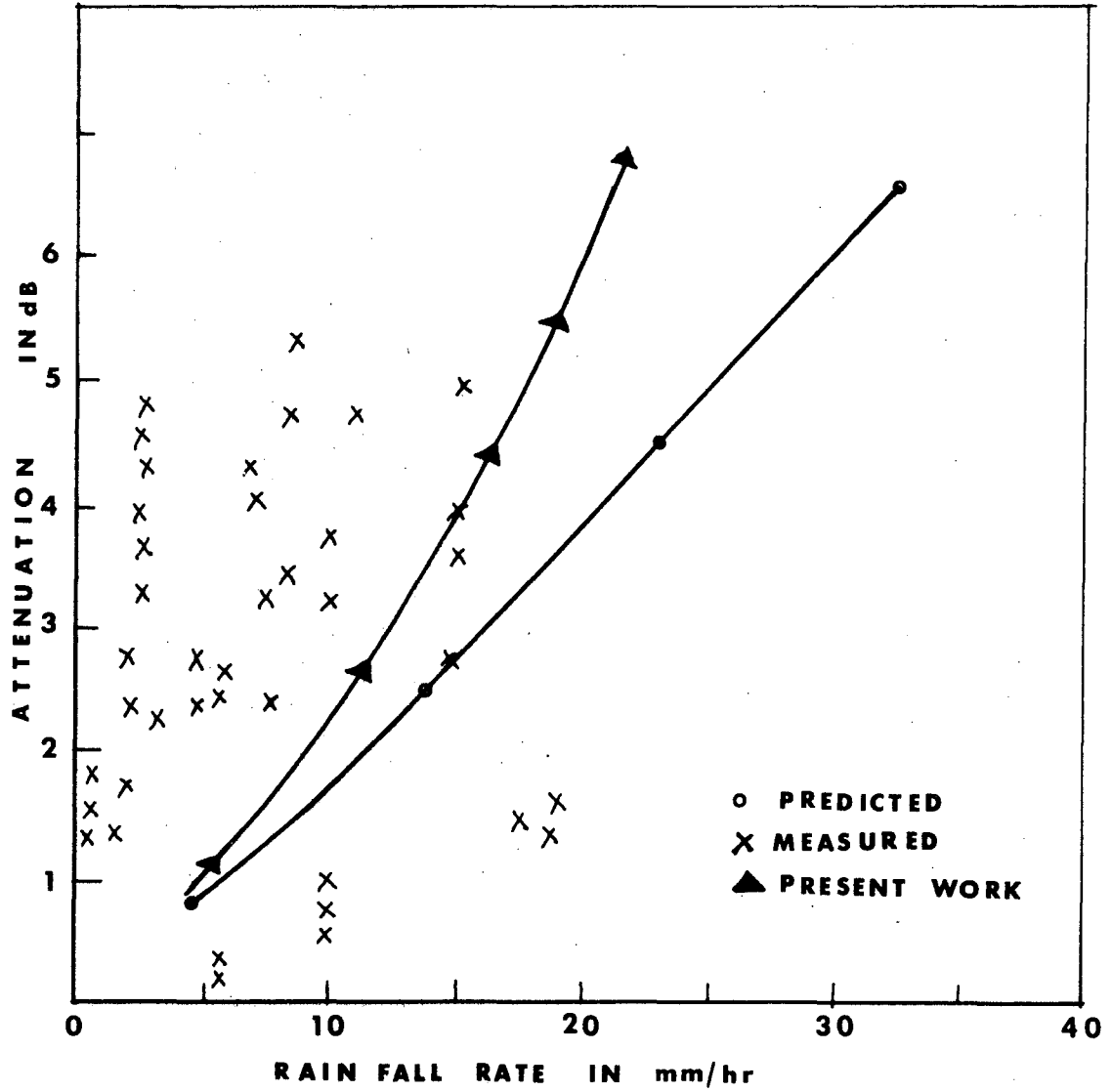
Figure 15. Comparison of Theoretical and Measured Rain Attenuation
for 15.3 GHz Space Link. (Measurements from ATS-V [63])
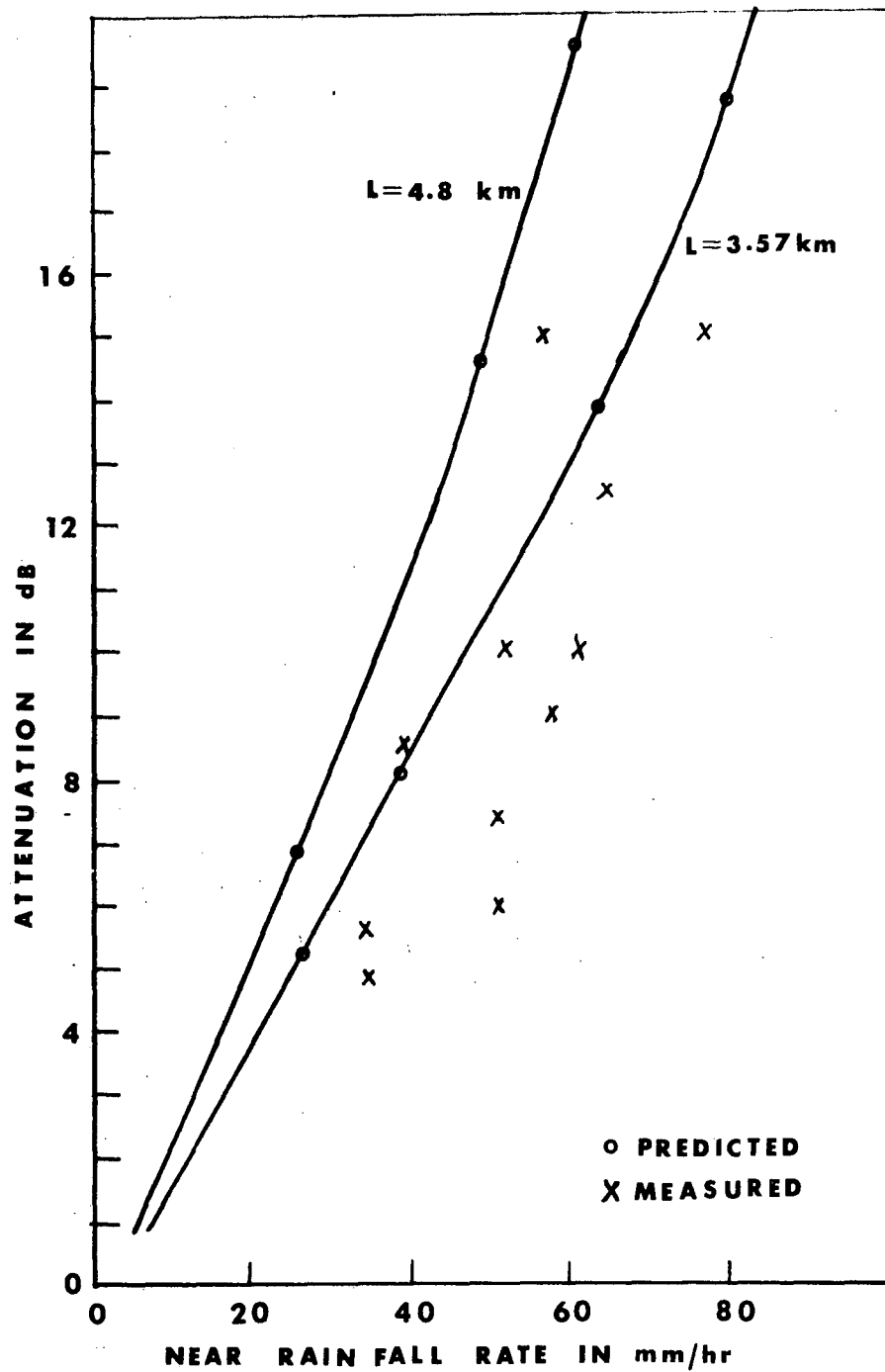
Figure 16(a). Theoretical and Measured Rain Attenuation for 15.3 GHz Space Link Versus Near Rainfall Rate. (Measurements from ATS-V [64])
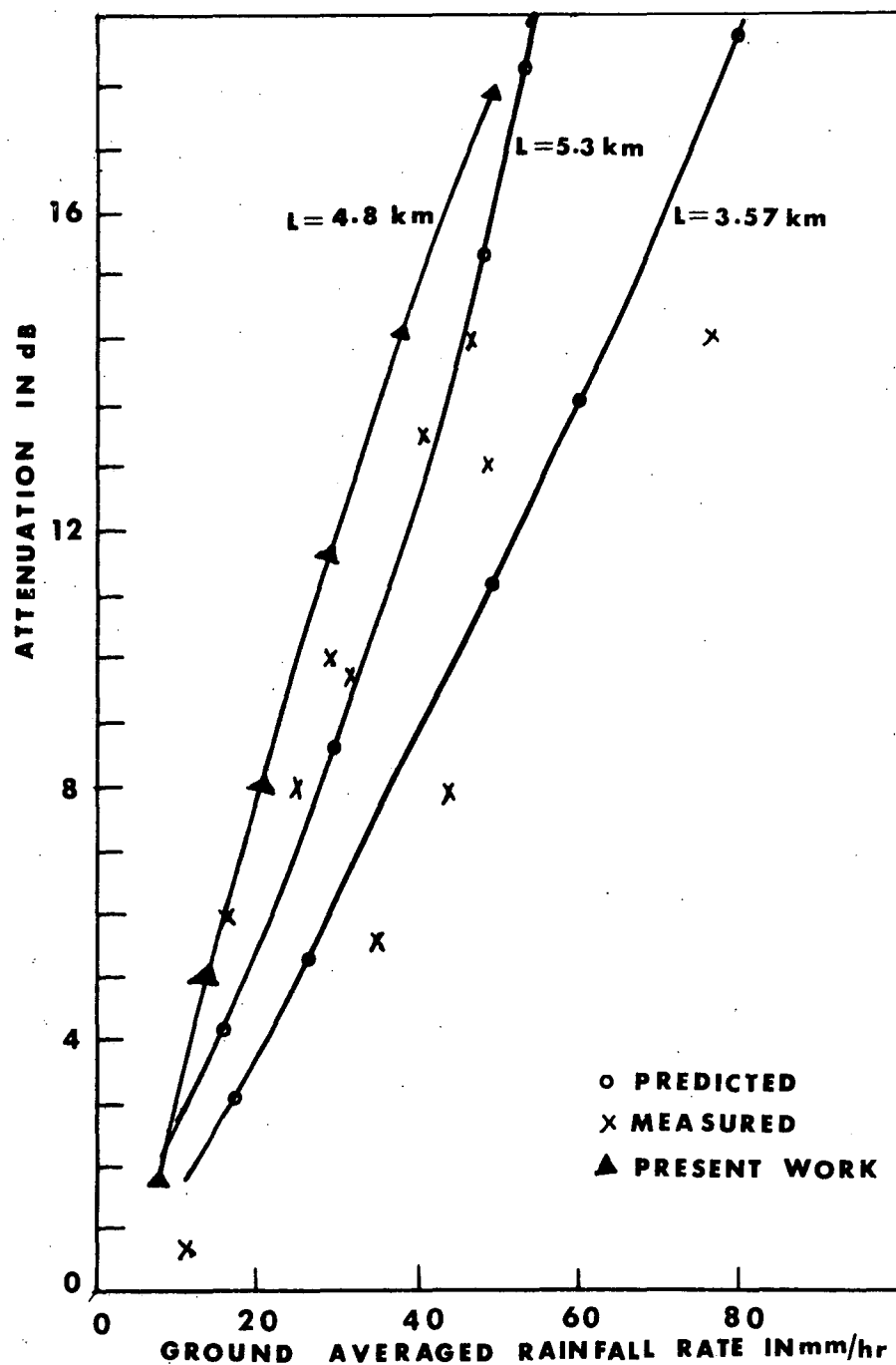
Figure 16(b). Theoretical and Measured Rain Attenuation for 15.3 GHz Space Link Versus Ground Averaged Rainfall Rate. (Measurements from ATS-V [64])
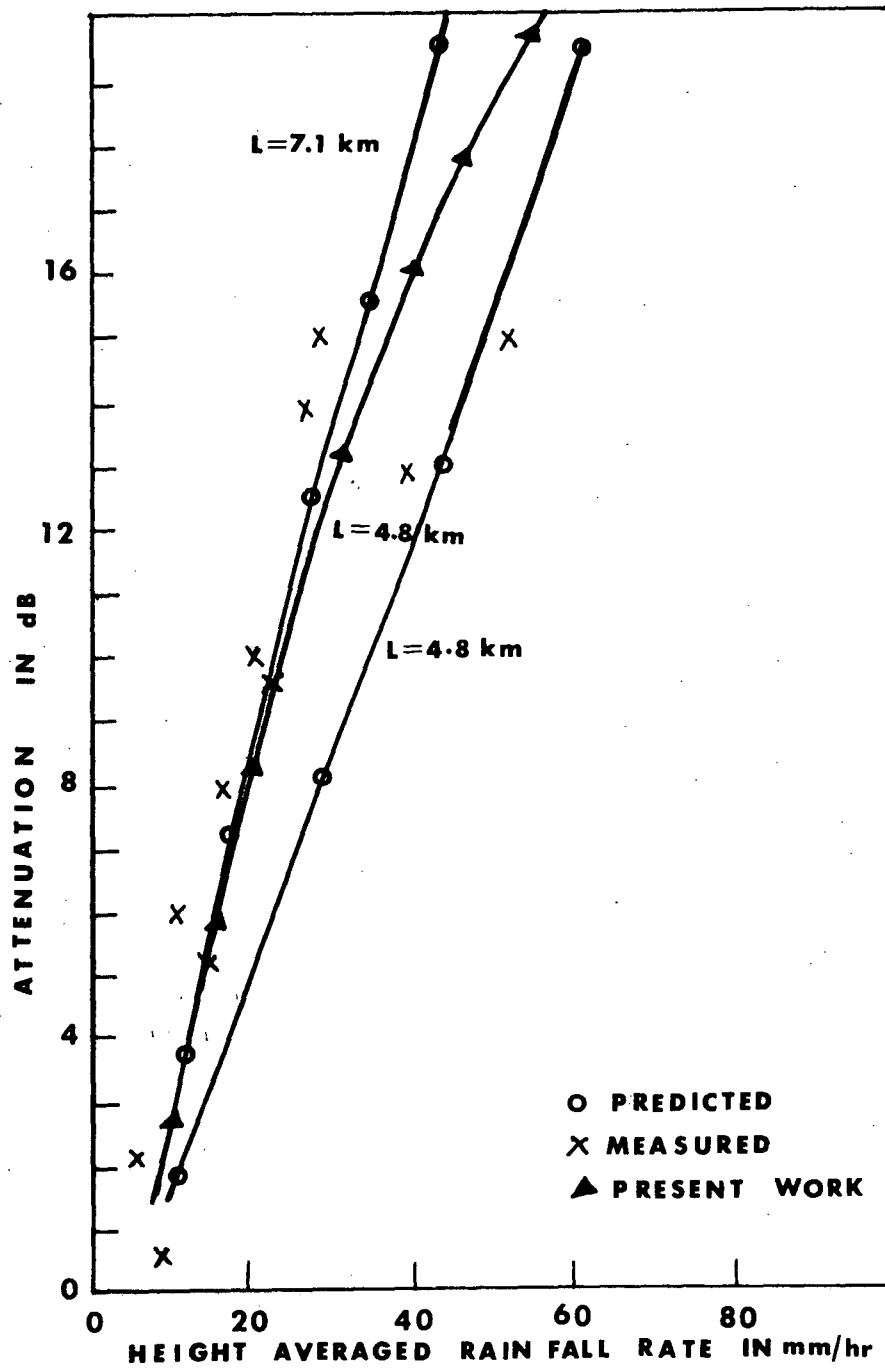
Figure 16(c). Theoretical and Measured Rain Attenuation for 15.3 GHz
Space Link Versus Height Averaged Rainfall Rate.
(Measurements from ATS-V [64])
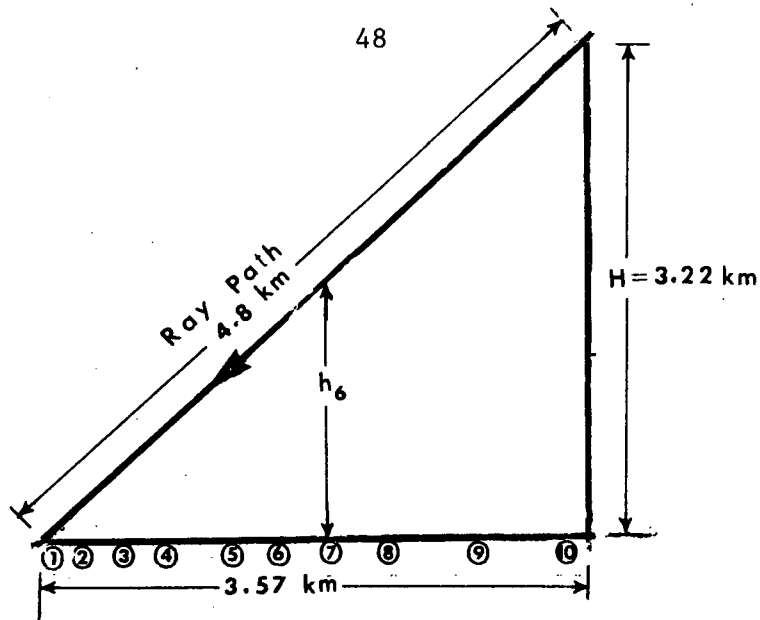
Figure 17. Rain gauge network at Roseman, N. C.[64]

Ippolito found that the reduction in dispersion between the

measured values and predicted values based on earlier theoretical

results, is most pronounced for $\overline{R}(h)$. However, the best fit prediction

curve for $\overline{R}(h)$, he found to be a slant path length of 7.1 km, which

corresponds to a vertical height of 4.73 km for rain path. Even

though the vertical height of rain path varies over wide limits,

it has been found that a model with a 3 km height is the most suitable

one [65]. With this assumption, the ray path length is taken as 4.8 km

and the results based on the new model are given in Figures 16 (b) and

(c). It is clear from (c) that the 4.8 km path attenuation based on

the new model versus height averaged rainfall rate gives the best

fit for the measured values.

V. SKY NOISE TEMPERATURE

Sources of noise in an idealized high gain antenna oriented skyward can be divided into two categories: those that exist outside the earth's atmosphere and those within the atmosphere.

(i) Outside the atmosphere, the sun, various radio stars, interstellar hydrogen, etc. radiate noise into the antenna. Also, very intense radiation originates near the center of our own galaxy.

(ii) Within our atmosphere, atmospheric gases and precipitation in addition to absorbing, also emit electromagnetic energy. Thus the atmosphere acts like an attenuator at some temperature T, and accordingly the oxygen, water vapor and precipitation within an antenna beam radiate noise into the antenna. The sum of these noise sources can be described by an effective noise temperature, which we call simply antenna temperature.

For a uniform medium in thermo-dynamic equilibrium, the theory of black body radiation states that a good absorber is also a good emitter (Kirchoff's Law). The atmosphere may be considered to approximate such a medium using Kirchoff's Law and the principle of conservation of energy, one can derive the radiative transfer equation, which describes the radiation field in the atmosphere that absorbs, emits and scatters energy. This field can be measured with an antenna, and for a non-scattering atmosphere the amount of radiation that is received when the antenna is pointed at a source [66] is,

$$T_a = T'_a e^{-\tau} + \int_0^{\infty} T(s)\gamma(s) \exp[-\int_0^{\infty} \gamma(s')ds']ds \quad . \tag{48}$$

T_a = Effective antenna temperature in °K

T'_a = Effective antenna temperature with no intervening atmosphere in °K.

τ = Total attenuation in nepers.

$\gamma(s)$ = Absorption coefficient.

s = Distance from antenna. (ray path)

In the above, T_a is proportional to the power received by the antenna. The first term on the right hand side represents direct energy from the source that has been attenuated by the atmosphere and the second term is the contribution resulting from noise radiated by the atmosphere. At mm wavelengths it can be assumed that discrete source (with the exception of sun and moon) and galactic emission are negligible. Thus, the first term becomes zero if the antenna is pointed away from the sun or the moon.

Hence an antenna observing the emitting medium would detect a received signal given by

$$\frac{P}{B} = \frac{k}{4\pi} \int_0^{4\pi} G(\Omega) \int_0^{\infty} T(s)\gamma(s) \exp[-\int_0^s \gamma(s')ds'] \ ds \ dr. \tag{49}$$

where P/B is the received power per unit frequency, P received power, B receiver bandwidth and $G(\Omega)$ the antenna gain function. Then we have,

$$T_a = \frac{P}{kB} = \int_0^\infty \int_0^{4\pi} \frac{G(\Omega)}{4\pi} T(s)\gamma(s)\exp[-\int_0^s \gamma(s')ds']dsdr \qquad (50)$$

$$T_a = \int^{4\pi} \frac{G(\Omega)}{4\pi} T_s(\Omega)d\Omega \approx \eta \, T_s(0) \qquad (51)$$

where the sky temperature

$$T_s(\Omega) = \int T(s)\gamma(s)\exp[-\int_0^s \gamma(s')ds']ds. \qquad (52)$$

and η = antenna efficiency.

Hence the antenna temperature or sky temperature for a given antenna may be computed once the attenuation coefficient and the temperature of the gas is known as a function of position.

A mean absorption temperature of the atmospheric path (T_m) may be considered, which is independent of frequency, and is related to the surface temperature T_g by,

$$T_m = (1.12 \, T_g - 50) \qquad \text{(where } T_m \text{ is in } °K \text{ and} \qquad (53)$$
$$T_g \text{ is in } °C)$$

Also a cosecant law for the attenuation and a total attenuation less than 1 dB, may be assumed. With these approximations, the equation for sky temperature becomes

$$T_s = T_s(0) \stackrel{\sim}{=} T_m \int_o^\infty \gamma(s) \exp[- \int_0^s \gamma(s')ds']ds \qquad (54)$$

$$T_s = T_m \left(1 - \exp[- \int_0^s \gamma(s')ds']\right) \qquad (55)$$

$$T_s = T_m(1 - \frac{1}{\alpha_T}) \qquad (56)$$

where α_T = total atmospheric attenuation.

Crane [55] has computed sky temperatures using the approximate equation (56) and compared with the measurements of Wulfsberg [67]. It is observed that the cosecant form of the approximation works well for elevation angles above 10° for 15 and 17 GHz and above 15° for 35 GHz.

The calculation of T_s from the above is generally limited to clear sky or thin cloud conditions since the assumptions in the derivation are not valid for appreciable condensed water absorption or scattering in the path. The ratio of the energy rescattered by the raindrop to that absorbed is called the single albedo. For small values of albedo most of the energy is absorbed and the incoherently scattered signal reaching the receiver will be negligible. Crane has computed values of single scattering albedo, using Laws and Parsons drop-size distributions, and has found that at frequencies below 12 GHz, the single scattering albedo is less than 0.2 for rains up to 6 in/hr. Hence it is concluded that at frequencies 12 GHz and below, the non-scattering medium transmission equation will be sufficient. Using this equation, Crane has computed sky temperatures at 7.78 GHz and compared with the measured

values and found that good agreement is obtained for rain when the estimated temperature change is in excess of 20°K. For lower estimated antenna temperatures, cloud effects are severe and no comparisons are made.

Wulfsberg and Altshuler [56] have determined rain attenuation at 15 and 35 GHz, from both extinction and emission measurements. The attenuation from emission measurement was calculated using the approximate formula given by (56). They have concluded that for orographic rain up to rates of 50 mm/hr in Hawaii, attenuations up to approximately. 10 dB can be calculated quite accurately from an emission measurement. Calculated attenuations at 15 and 35 GHz using emission measurement are found to be in fairly good agreement with those obtained using the sun as a source with correlation coefficients of 0.98 and 0.97, respectively.

Falcone [25] has found that by increasing the oxygen line-breadth constant from 0.02 to 0.025, the calculated values of apparent sky temperature from the radiative transfer equation are in good agreement with the measured values at 15, 17 and 35 GHz. However, these results are for fair weather conditions only.

Hogg [68] has computed the effective antenna temperatures due to oxygen and water vapor in the atmosphere for the frequency range 0.5 to 40 GHz, using the International Standard Atmosphere model. It may be extrapolated from his results, that effective temperature at 12 GHz

increases from about 3° to 120°K due to oxygen, and 1° to 100°K due to water vapor as the Zenith angle is increased from 0° to 90°.

The effect of clouds on the apparent sky temperature depends on their height, thickness, and water content. Cirrus clouds composed of ice crystals, produce a negligible contribution to sky noise. Wulfsberg [67] has found that the increase in Zenith temperatures due to large fair-weather cumulus clouds to range from 5°K to 25°K at 35 GHz. and only a few degrees at 15 GHz.

Ippolito [63] has shown the attenuation predicted from sky temperature measurements at 16 GHz using the simplified formula, as compared with the measured attenuation from ATS-V experiment for four hours of rain storm. The correlations of these vary from hour to hour, with the best prediction occurring during the heaviest recorded ground rainfall. This result is termed as a surprise, however the same results have been found from other measurements of ATS-V [64]. It may be noted that Crane's results also support this kind of observation, in that correlation between predicted and measured values appears better at higher levels of attenuation.

Based on these results, it is concluded that sufficiently accurate results will be obtained by computing the sky temperatures based on the simplified formula (56).

VI. STATISTICAL ANALYSIS

The atmospheric attenuation and the corresponding sky noise temperature have been found to be highly weather-dependent. Hence statistical data on the levels of these is required in order to specify the long term performance of the TVBS System. The statistical meteorological approach has the advantage that results are obtained with much less expense and effort than would be required in an experimental approach.

Five typical locations in the United States are selected for the weather statistics. These are Washington, D. C., Albany (New York), Montgomery (Alabama), Miami (Florida) and Sacramento (California). The weather information at these places is obtained for 7 p.m. (EST) each day during the year 1970, from Local Climatological Data, a U. S. Department of Commerce publication. Such a sampling is expected to reflect with sufficient accuracy the time and space variations for all temperate regions.

For a given path, attenuation due to oxygen is assumed constant, since daily or seasonal changes in pressure or temperature alter the oxygen concentration negligibly. Further, at 2.5 GHZ, the attenuation due to water vapor, clouds and rain is negligible and hence the statistical analysis is needed only for 12 GHZ.

Water vapor density in the atmosphere is most directly related to the dew point temperature. This relation given by Berry, et al. [69] is shown in Figure 18.

The effect of clouds on attenuation depends on their height, thickness and water content. Clouds come in a variety of sizes, shapes and textures. When one studies the appearance of clouds, it becomes apparent that there are distinct types. On this basis, one could group them into three fundamental classes; stratus, cumulus and cirrus. Some differentiating characteristics of these clouds as given by Mason [70] are shown in Table 3. The water content are the averages of those listed by Fletcher [71]. The type of cloud on each day is identified by the ceiling height given in climatological data sheet. The temperature of the cloud is approximately estimated from the Pseudo-Adiabatic Diagram of the weather bureau.

The rain statistics are taken from the hourly average value given in climatological data at 7 p.m. (EST). Bussey [72] has found, that on the average, about 20% of the time during an hour was really time of zero rate or of the very low rate known at 'trace,' about 35% of the time the mean hourly rate was exceeded, and to exceed it by 5 or 6 times for a few minutes was a fairly common occurrence. He has also derived that 1 hour point rates give instantaneous 50 km path rates. This assumption is used in the present work.

From the above statistics, computations have been made to determine time and space variations of attenuation and receiver noise
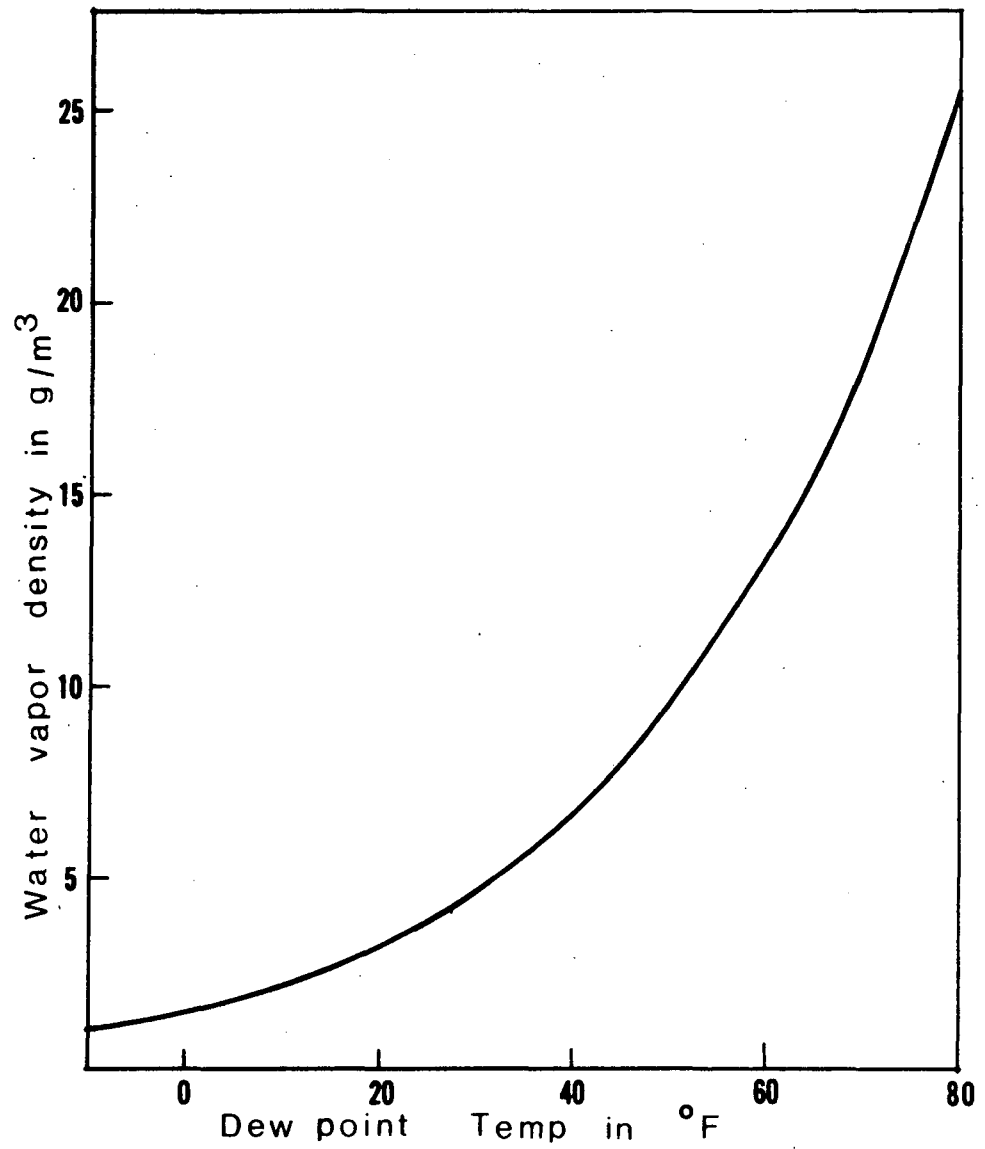
Figure 18. Water Vapor Density Versus Dew Point Temperature. (Data from Berry, et al. [69])

TABLE 3 - PRINCIPAL CLASSES OF CLOUDS IN TEMPERATE REGIONS (Data from [70])

TYPE	CEILING RANGE	WATER CONTENT	TEMP-ERATURE	VERTICAL HEIGHT	CHARACTERISTICS
I. STRATIFORM					
a) High Level. (i) Cirrus (Ci) (ii) Cirro-cumulus (Cc) (iii) Cirro-stratus (Cs)	5 to 13 km.	very small	$-25°C$	only a few hundred feet thick	composed of ice crystals.
b) Medium Level. (i) Alto-stratus (As) (ii) Alto-cumulus (Ac)	2 to 7 km.	0.15 g/m^3	0 to $-25°C$	about 4 km.	composed of mainly water droplets. Rain or snow may fall from As. The atmosphere is often hazy just below Ac.
c) Low Level. (i) Strato-cumulus (Sc) (ii) Stratus (St) (iii) Nimbo-stratus (Ns)	Sc is below 2 km. St and Ns usually within 0.3 to 0.6 km of the ground	0.25 g/m^3	usually warmer than $-5°C$	about 2 km	Composed of water droplets gives drizzle.

TABLE 3.   CONTINUED

TYPE	CEILING RANGE	WATER CONTENT	TEMP-ERATURE	VERTICAL HEIGHT	CHARACTERISTICS
II. CUMULIFORM.					
(i) Cumulus (Cu)	0.6 to 6 km or more	0.38 g/m^3	-	about 6 km	Thick, scattered, develops on days of clear skies. Water cloud.
(ii) Cumulo-nimbus (Cb)	up to 12 km	0.45 g/m^3	may be as cold as -50°C		Cb generally produces showers of rain or snow, sometimes hail, soft-hail, or thunder-storms.

temperature. The computer program for time variation analysis for one sample is as shown in Appendix A. Five samples are taken for time variation analysis and six samples are chosen for space variation analysis. The corresponding values for an elevation angle of 90° are shown in Table 4 and Table 5. The overall averages of all samples are shown in Table 6, for 8 elevation angles. Cumulative distributions for vertical attenuation due to oxygen and water vapor, clouds, precipitation, and for total attenuation at all five locations are shown in Figures 19, 20, 21 and 22, respectively. The cumulative distribution for the apparent sky temperature are shown in Figure 23.

The effects of different elevation angles for the ray path on the total attenuation and the corresponding sky noise temperature are shown in Figures 24 and 25, respectively. Though these are for New York type weather, they may be taken as representative for all temperate regions.

61

TABLE 4 – RESULTS OF STATISTICAL ANALYSIS (TIME VARIATION)
FOR 90° ELEVATION ANGLE. (7 P.M. EST each day during 1970)

WEATHER TYPE	TOTAL ATTENUATION (dB)			SYSTEM NOISE TEMP (dB/°K)		
	MEDIAN	MEAN	STANDARD DEVIATION	MEDIAN	MEAN	STANDARD DEVIATION
Washington, D.C.	0.1682	0.2240	0.1387	30.740	30.749	0.0293
Montgomery, Al.	0.1776	0.2425	0.4505	30.743	30.757	0.1221
Albany, NY	0.1663	0.2156	0.1426	30.738	30.746	0.0294
Miami, Fl.	0.1880	0.2494	0.1662	30.746	30.757	0.0368
Sacramento, Ca.	0.1338	0.1732	0.1089	30.733	30.739	0.0228
TOTAL	0.8339	1.1047	1.0078	153.700	153.748	0.2404
AVERAGE OF ALL SAMPLES	0.1668	0.2209	0.2016	30.740	30.750	0.0481

TABLE 5 – RESULTS OF STATISTICAL ANALYSIS (SPACE VARIATION) FOR 90° ELEVATION ANGLE (7 P.M. EST at five locations)

TIME 7 P.M. (EST) ON	STD. DEVIATION OF TOTAL ATTENUATION (dB)	STD. DEVIATION OF SYSTEM NOISE TEMP (dB/°K)
Jan. 1, '70	0.1554	0.0329
Mar. 1, '70	0.1449	0.0304
May 1, '70	0.1213	0.0267
July 1, '70	0.0347	0.0076
Sept. 1, '70	0.0846	0.0194
Nov. 1, '70	0.1112	0.0226
TOTAL	0.6521	0.1391
AVERAGE	0.1087	0.0232

TABLE 6 — TIME AND LOCATION PROBABILITY DATA.
(7 P.M. EST each day during 1970 for 5 locations)

ELEVATION ANGLE (DEGREES)	TOTAL ATTENUATION (dB)			SYSTEM NOISE TEMP. DATA (dB/°K)		
	MEDIAN $F_d(50,50)$	STD. DEVIATION σ_{td}	STD. DEVIATION $\sigma_{\ell d}$	MEDIAN $F_u(50,50)$	STD. DEVIATION σ_{tu}	STD. DEVIATION $\sigma_{\ell u}$
90.0	0.1668	0.2016	0.1087	30.740	0.0481	0.0232
78.0	0.1705	0.2060	0.1112	30.740	0.0489	0.0238
66.5	0.1819	0.2198	0.1186	30.743	0.0515	0.0252
55.0	0.2036	0.2460	0.1327	30.750	0.0564	0.0279
43.7	0.2413	0.2917	0.1574	30.756	0.0643	0.0326
32.7	0.3084	0.3730	0.2012	30.771	0.0773	0.0404
22.0	0.4436	0.5379	0.2902	30.799	0.0999	0.0549
11.7	0.8098	0.9936	0.5356	30.873	0.1453	0.0864
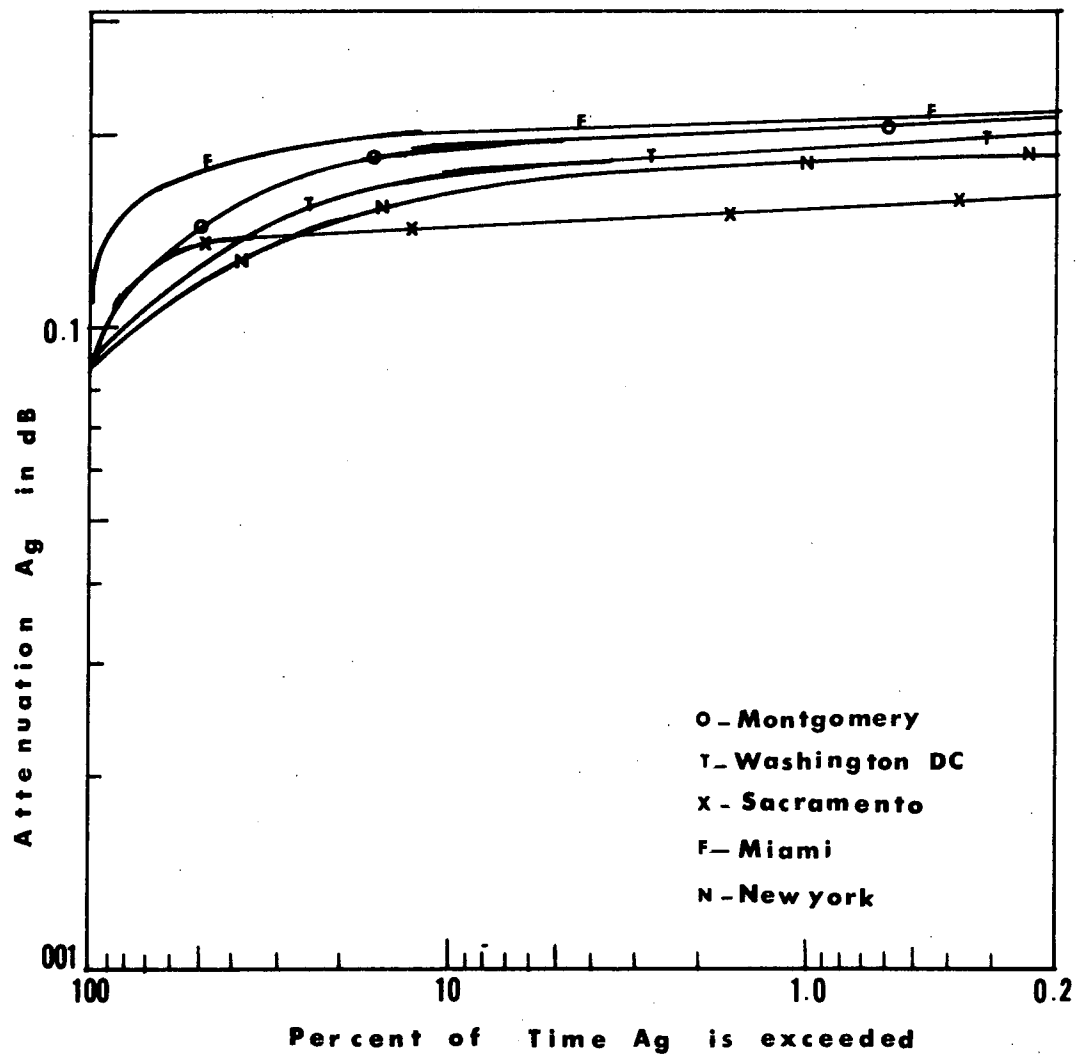
Figure 19. Cumulative Distributions for Vertical Attenuation due to Oxygen and Water Vapor at Different Locations.
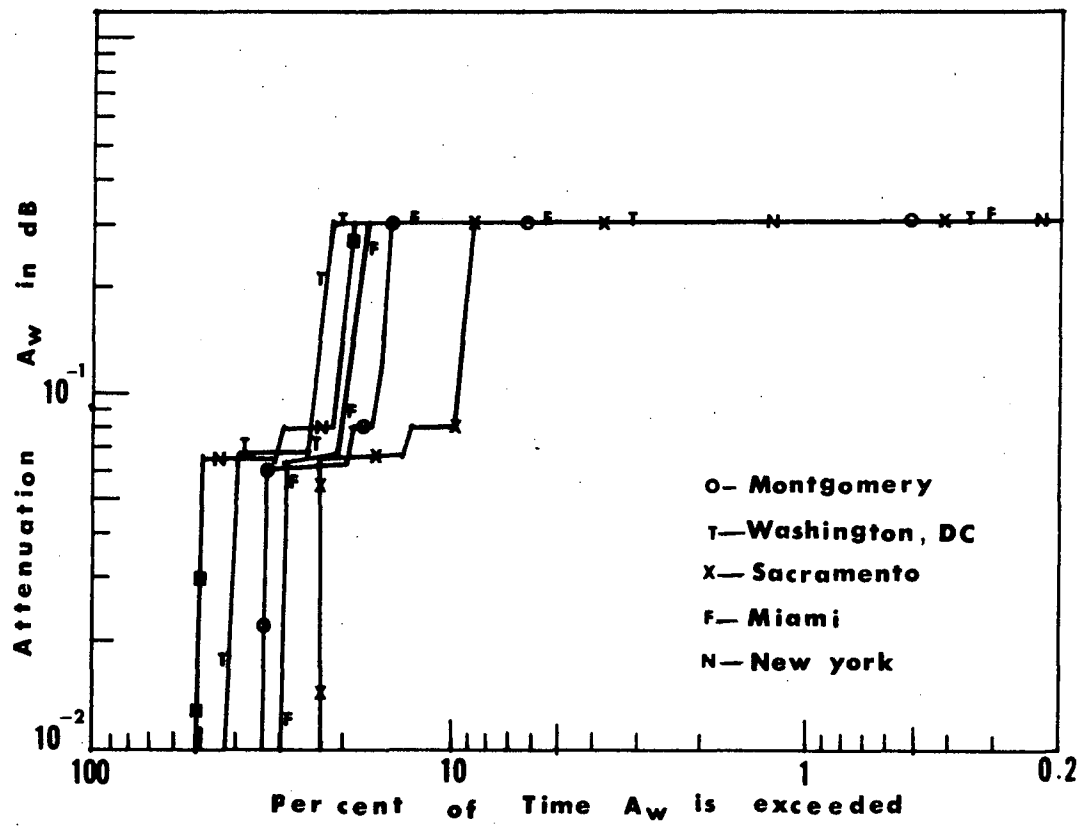
Figure 20. Cumulative Distributions for Vertical Attenuation due to Clouds at Different Locations.
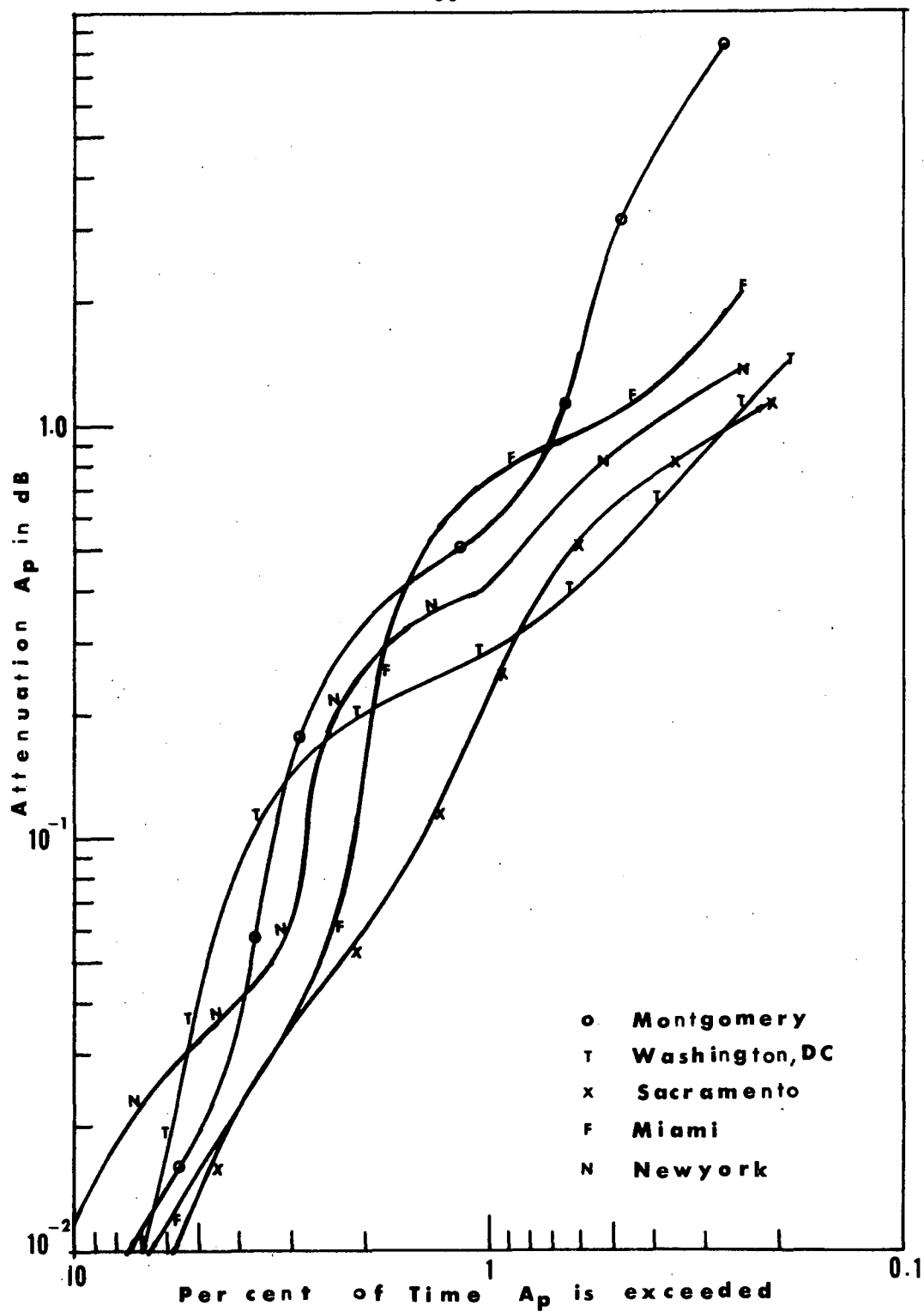
Figure 21. Cumulative Distributions for Vertical Attenuation due to Rain at Different Locations.
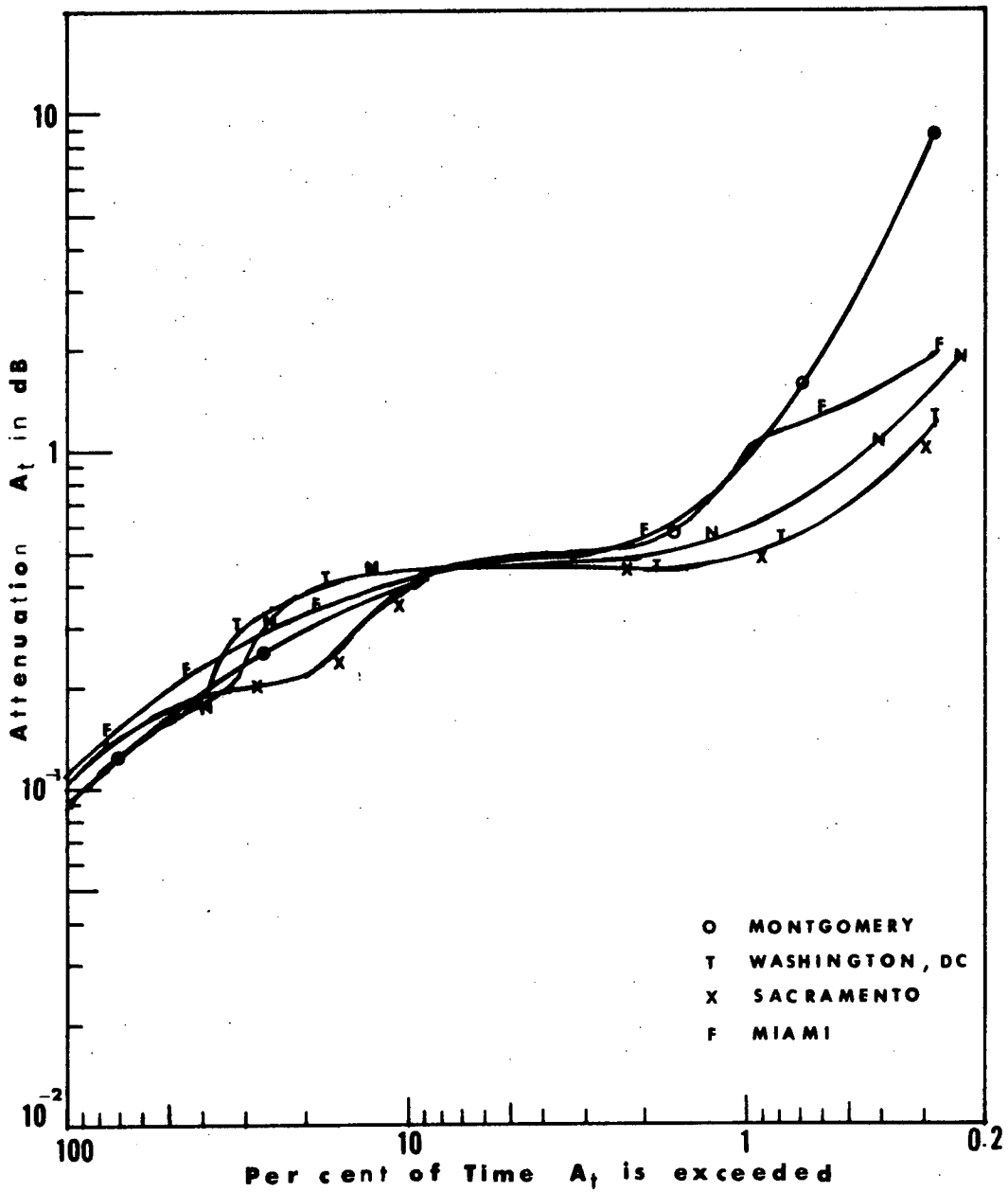
Figure 22. Cumulative Distributions for Total Vertical Attenuation
at Different Locations.
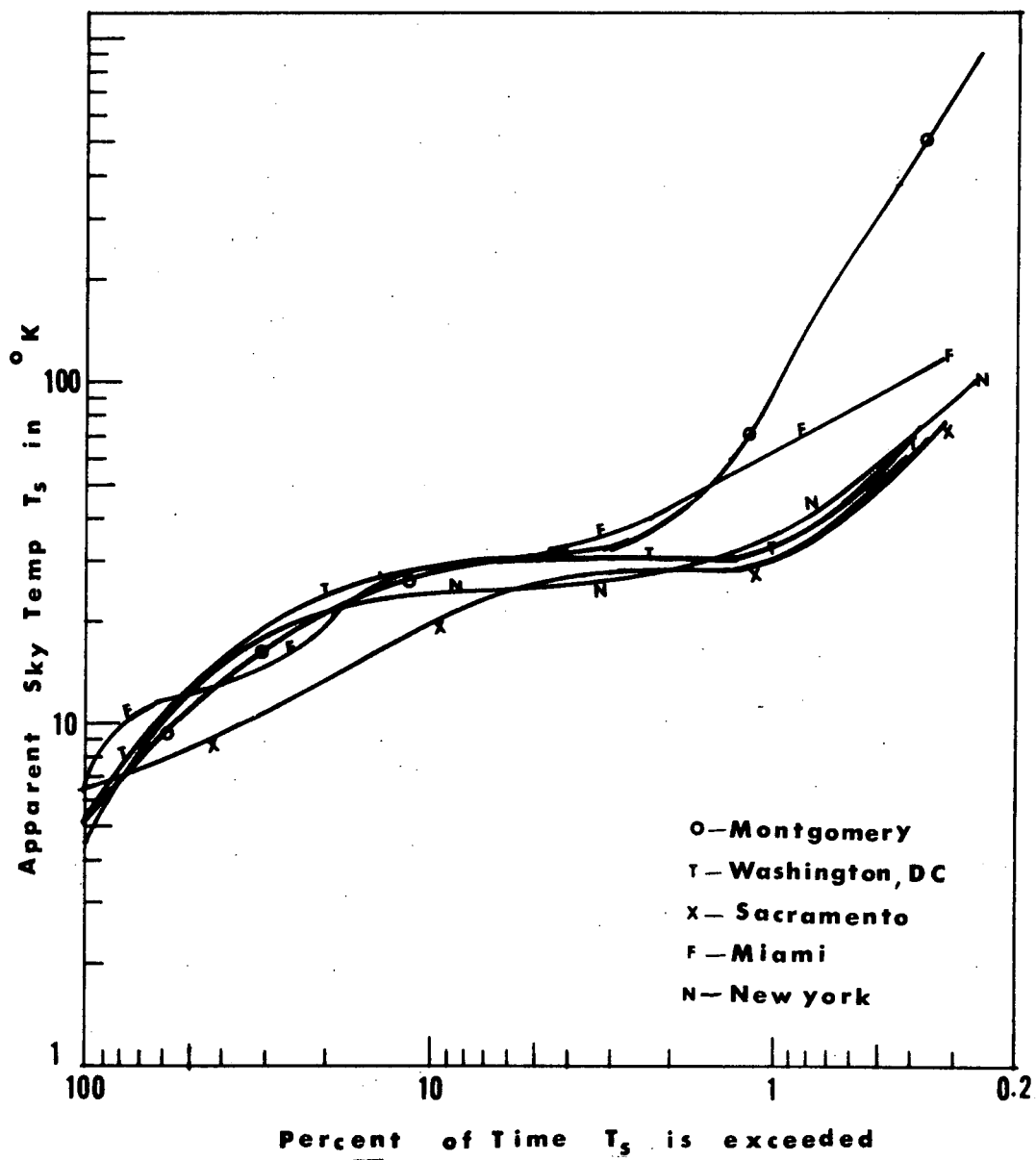
Figure 23. Cumulative Distributions for Apparent Sky Temperature due to Vertical Attenuation at Different Locations.
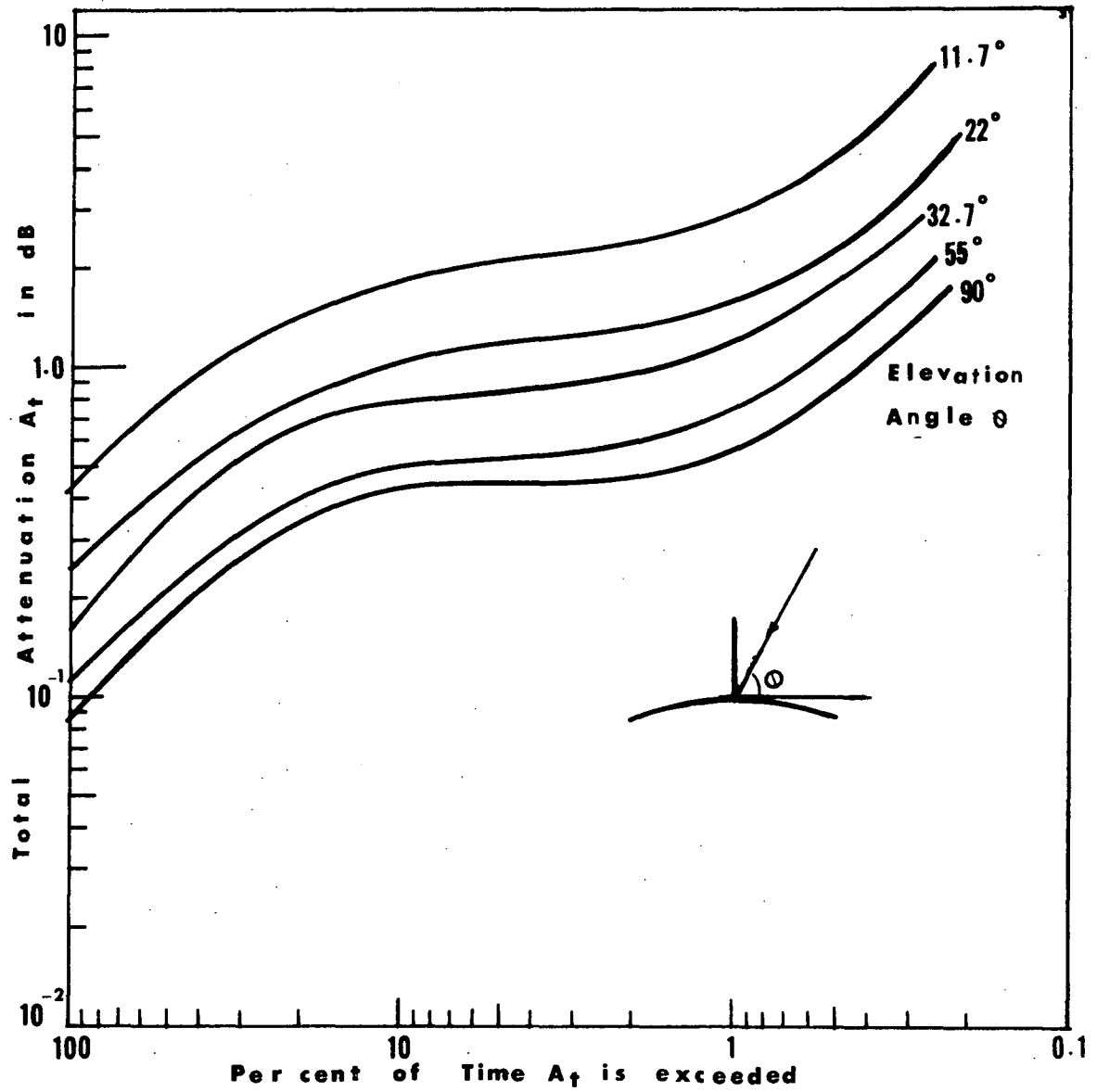
Figure 24. Cumulative Distributions for Total Attenuation at Various Elevation Angles and New York Type Weather.
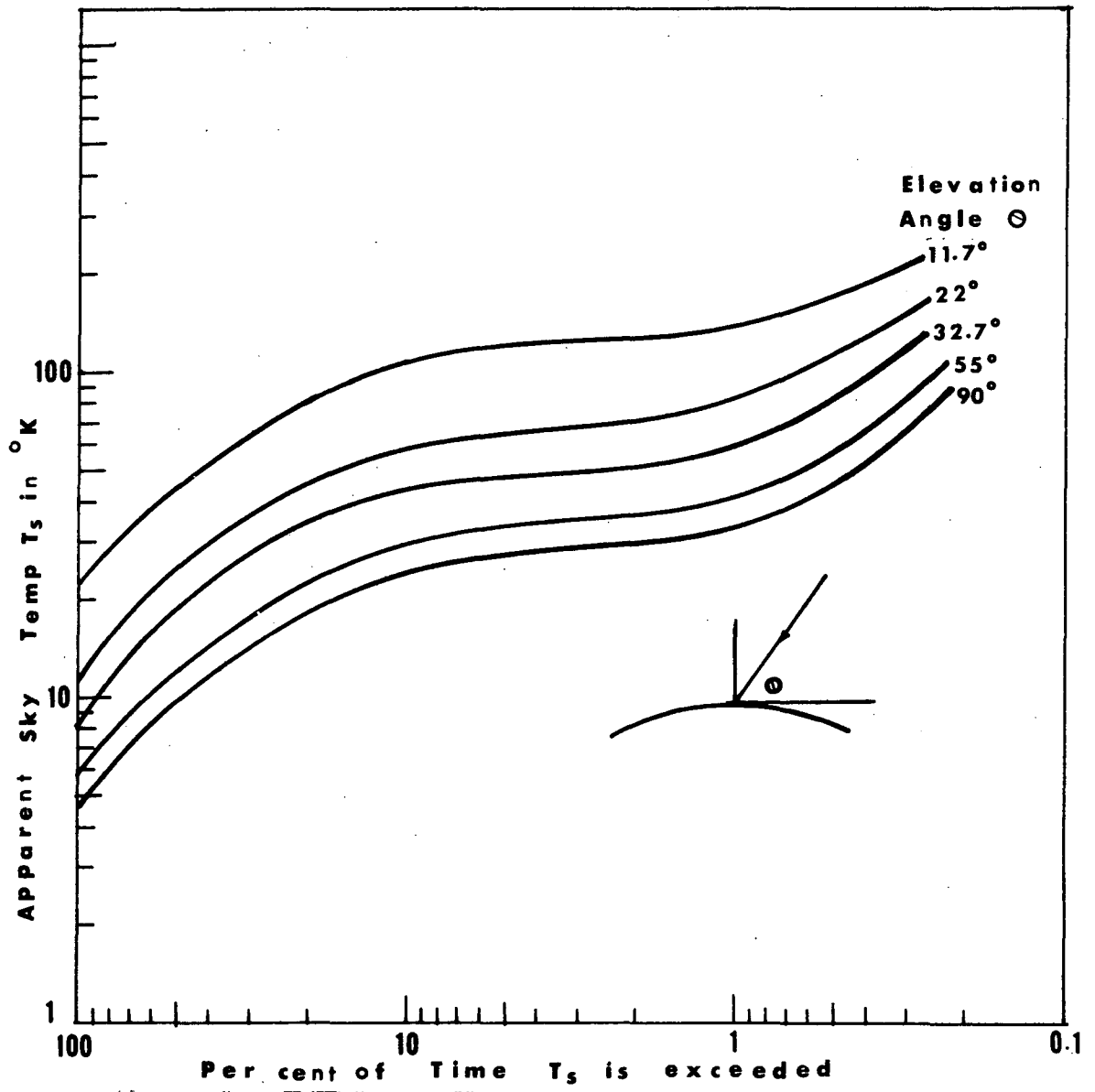
Figure 25.   Cumulative Distributions for Apparent Sky Temperature at
Various Elevation Angles and New York Type Weather.

VII. PICTURE QUALITY

In any broadcast system, it is desirable that means exist for estimating how large an area can be reached by its programs and to know how quality of reception varies over this area. In the Final Report of TASO [22], it has been recommended to the FCC that one has essentially three basic qualities to specify in characterizing a level of Television Service: (1) level of picture quality to be achieved or exceeded; (2) the grade of receiver plant postulated for the observation of picture quality; and (3) the time and location probabilities $F(L,T)$ of receiving at least that level of picture quality. Two methods of approaching this problem of specifying level of service were considered by TASO. These are (1) the location probability method; and (2) the acceptance ratio method. The location probability method has been used by FCC in its allocation and channel assignment operations. This method, also recommended by the study group XI of the CCIR XIIth plenary assembly [73], may be modified as follows for space broadcasting.

The protection ratio is usually defined as the minimum permissible power ratio of the wanted-to-interfering signals available at the receiver input to provide the desired quality grade of service. The interfering signal in case of satellite broadcasting is only random noise, since co-channel and adjacent channel interferences are assumed non-existing. Hence it is simpler to define the protection ratio in

71

terms of the ratio of the carrier power in watts to system noise
temperature in degree Kelvin. Then the television service to a re-
latively small area may be described by the following algebraic-
statistical equation.

$$R(Q) = F_d(50,50) - F_u(50,50) - H(T) - H(L) \tag{57}$$

where $\quad H(T) = k(T) \sqrt{\sigma_{td}^2 + \sigma_{tu}^2}$ $\qquad$ (58)

$$H(L) = k(L) \sqrt{\sigma_{\ell d}^2 + \sigma_{\ell u}^2} \tag{59}$$

$R(Q)$ = Protection ratio of wanted-to-interfering signal, in dBW/°K,
at the receiver input required to provide a service quality Q
under non-varying conditions. Subscripts d and u refer to the
wanted and unwanted signals, respectively.

$F_d(50,50)$ = Median value of carrier power in time and location, in
dBW.

$F_u(50,50)$ = Median value of system noise temperature in time and loca-
tion, in dB/°K.

$k(x)$ = Standard normal variate.

$$k(50) = 0, \; k(70) = -0.525, \; k(90) = -1.282 \tag{60}$$

σ_t = Standard deviation with time

σ_ℓ = Standard deviation from location to location.

For the purpose of describing service, the above equation may be interpreted as follows: If service of quality grade Q is defined to be available at a given location only when the protection ratio at the receiver input exceeds the required value R(Q) - i.e., the non-varying protection ratio is exceeded for T% of the time, then in this area, at least L% of the locations will have this quality of service Q. The following assumptions are made in the Equation (57).

(1) The receiving antenna gain is same for both wanted and un-wanted signals and the variability in gain throughout the area is negligible.

(2) The two signals have approximately Gaussian distributions both in time and with location.

(3) Both the time correlation and location correlation between the desired and interfering signals are negligible.

It may be seen from the above, that there are three interdependent parameters needed to describe the service to the area - i.e., Q, L, T. It has been standardized that a particular service area has a satis-factory picture quality Q, when T has a value of 90% and L has a value of 70%. Based on these, boundaries of iso-service contours may be drawn to depict the coverage of the broadcasting station. In order to make the method applicable on a world wide basis to any system design for temperate regions, the following procedure is adopted.

Contours of equal elevation angle on the surface of the earth for a given position of satellite are drawn on the Figure 26. This may
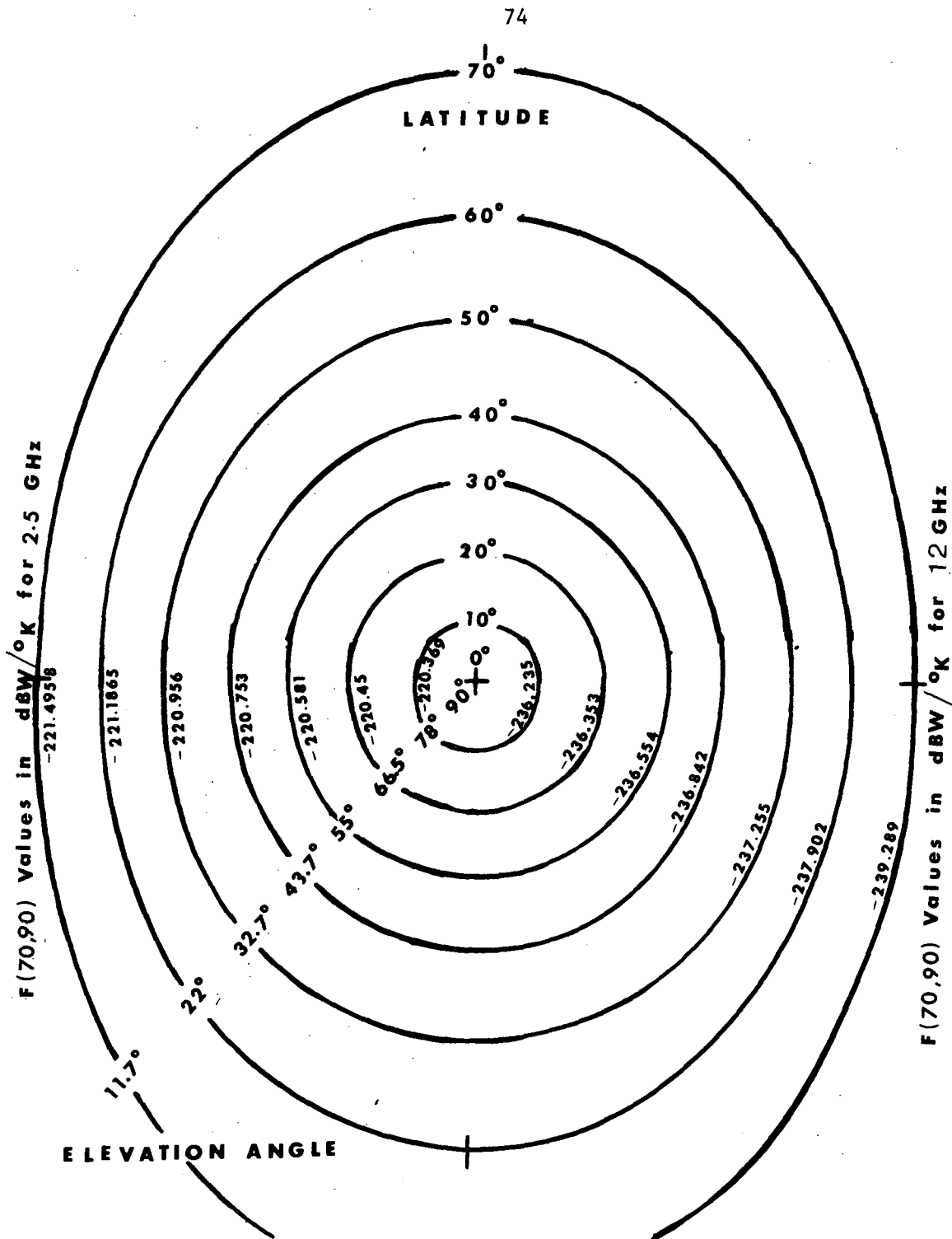
Figure 26. Contours of Equal Elevation Angle and the Corresponding
F(70,90) Values at 2.5 and 12 GHz.

be used by positioning it in the east-west direction according to the longitudinal location of the synchronous satellite (satellite position is denoted by the + in the center of the figure). The north-south position is aligned with the equator. Use of this figure for a particular example is illustrated in Figure 27. The satellite transmitter output power is assumed to be 1 watt and the transmitting and receiving antenna gains are at isotropic level. Then the median value of the desired signal at the input of a receiver situated at a given elevation angle on the surface of the earth is given by the sum of the free space loss and the median value of the total attenuation. The free space loss is given by

$$L_{FS} = (92.45 + 20 \log_{10}f + 20 \log_{10}R)dB \qquad (61)$$

where f = Frequency in GHZ

    R = Slant range of ray path in km.

$$= [r_o^2\sin^2\theta + R_V(2r_o + R_V)]^{1/2} - r_o\sin\theta \qquad (62)$$

    r_o = Radius of earth (6378 km)

    R_V = Vertical height of satellite (35,200 km)

    θ = Elevation angle, in degrees.

The median value of the undesired signal is the median value of system noise temperature. From these values and the standard deviations

SP — SATELLITE POSITION
AP — SAT. ANT. BEAM CENTER
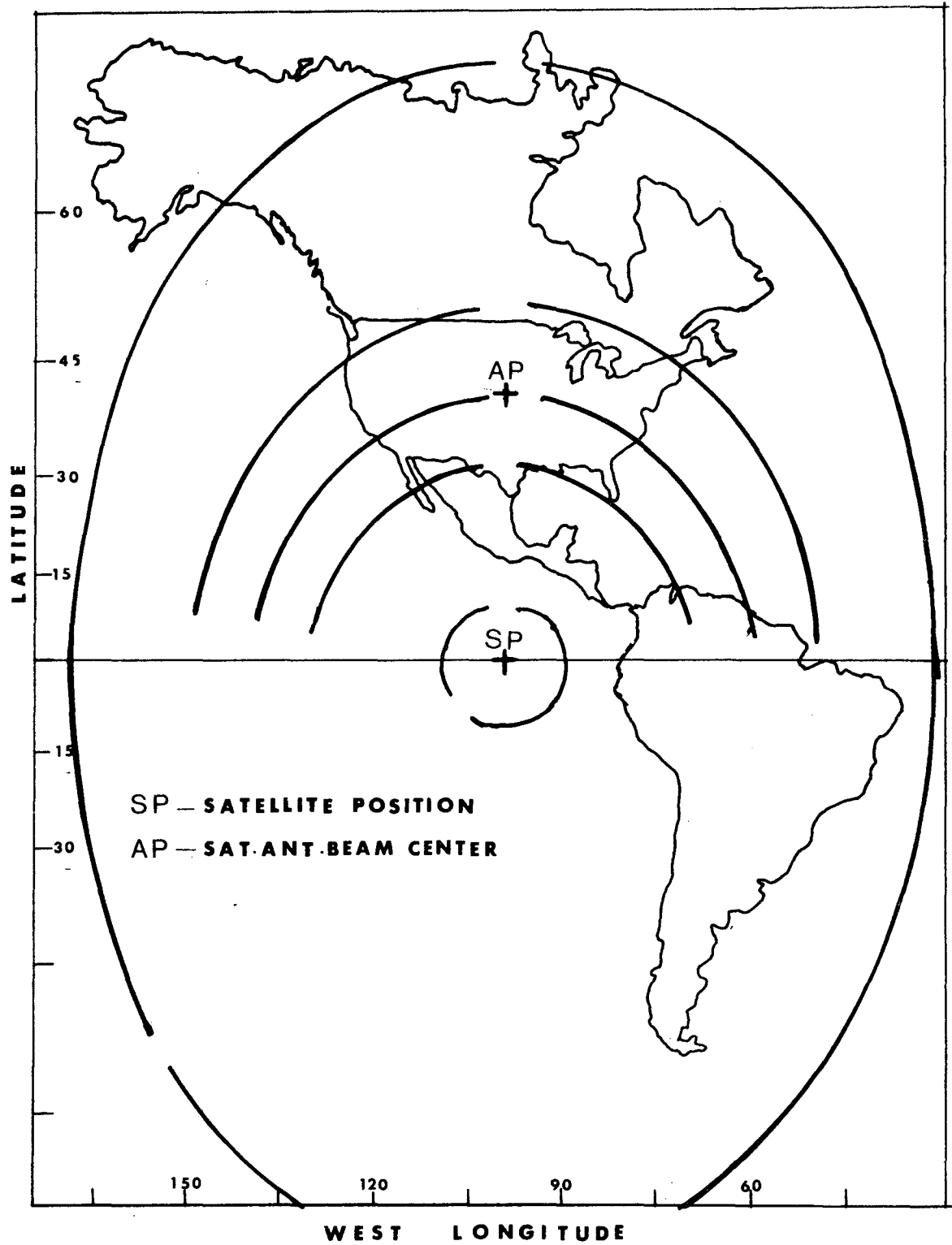
Figure 27. Use of Figure 26 for a Particular System Example.

determined earlier, the F(70,90) values of dBW/°K are determined for

12 GHz and are as shown in Figure 26. The corresponding values at

2.5 GHz are, of course, non-time varying and are also shown in Figure 26.

(The system noise temperature assumed for 2.5 GHz is 800°K, whereas

for 12 GHz the receiver noise figure is assumed to be 7 dB). The use

of Figure 26 for a particular system design is explained in the next

chapter.

Now with regard to the numbers to be specified for grades of

picture quality, TASO numbers seem to be the most appropriate ones

since these are the results of most extensive investigations made so

far. The TASO numbers are carrier-to-noise ratios at the RF input of

AM/VSB 525-line television receiver, and hence are to be modified

for FM case. Unfortunately, adequate data on the correlation

between subjectively experienced picture quality and signal-to-noise

ratio are not available for FM transmission. Therefore, the best

approach is to convert the carrier-to-noise ratios in the TASO's tests

to weighted-picture-SNR's. Further, it may be assumed that FM trans-

mission with a given weighted-picture-SNR would rate the same sub-

jective grade in a viewer panel test as AM transmission with the same

weighted-picture-SNR. These picture-SNR's are then to be converted

back into carrier-to-noise ratios for the particular FM standard used

for satellite broadcasting. Based on a minimum power design procedure,

TRW systems [1] have made these conversions, and the same are given

for 625 line, color FM transmission with 5.5 MHZ video bandwidth in

Table 7. The (C/T) values are shown only for fine and passable quality,

since these are the most relevant for satellite broadcasting.

TABLE 7 - PICTURE QUALITY GRADES

TASO GRADE	NAME	TASO CARRIER-TO-NOISE RATIO (dB) [22]	WEIGHTED PICTURE-SNR (dB) [1]	F.M. TRANSMISSION [1]	
				CARRIER-TO-NOISE TEMP RATIO (dBW/°K)	R.F. BAND-WIDTH (MHZ)
1	EXCELLENT	46	49.5	–	–
2	FINE	38	40.3	–139.0	22.8
3	PASSABLE	31	32.2	–140.5	16.0
4	MARGINAL	25	25.9	–	–
5	INFERIOR	19	19.9	–	–

VIII. SYSTEM DESIGN

An example of a Satellite Broadcasting System is assumed to
illustrate the procedure of obtaining boundaries of picture quality
contours. The area of coverage assumed is the central United States.
The satellite is positioned at 100° west longitude and the satellite
antenna beam axis is pointed to 100° west longitude and 40° latitude
position as shown in Figure 27. The satellite antenna chosen is a
parabolic circular aperture, with a tapered illumination (n = 1),
and with an aperture diameter of 27 wavelengths. The antenna gain
versus angle off beam center for such an antenna is computed and shown
in Figure 28. (The pattern for uniform illumination is also shown in
this figure for comparison). Contours of equal antenna gain on the
earth surface are now estimated and are as shown in Figures 29 and 30.
The ground receiving antenna is assumed to be a parabola of 1 meter
aperture diameter. This results in a gain of 25.76 dB for 2.5 GHz and
39.40 dB for 12 GHz.

Now the down-link power budget for a particular location on the
surface of the earth may be expressed by the following:

$$(C/T) = TP + (SNT + TPL) + SAG + RAG + (ULN + PL + CL) \qquad (63)$$

where
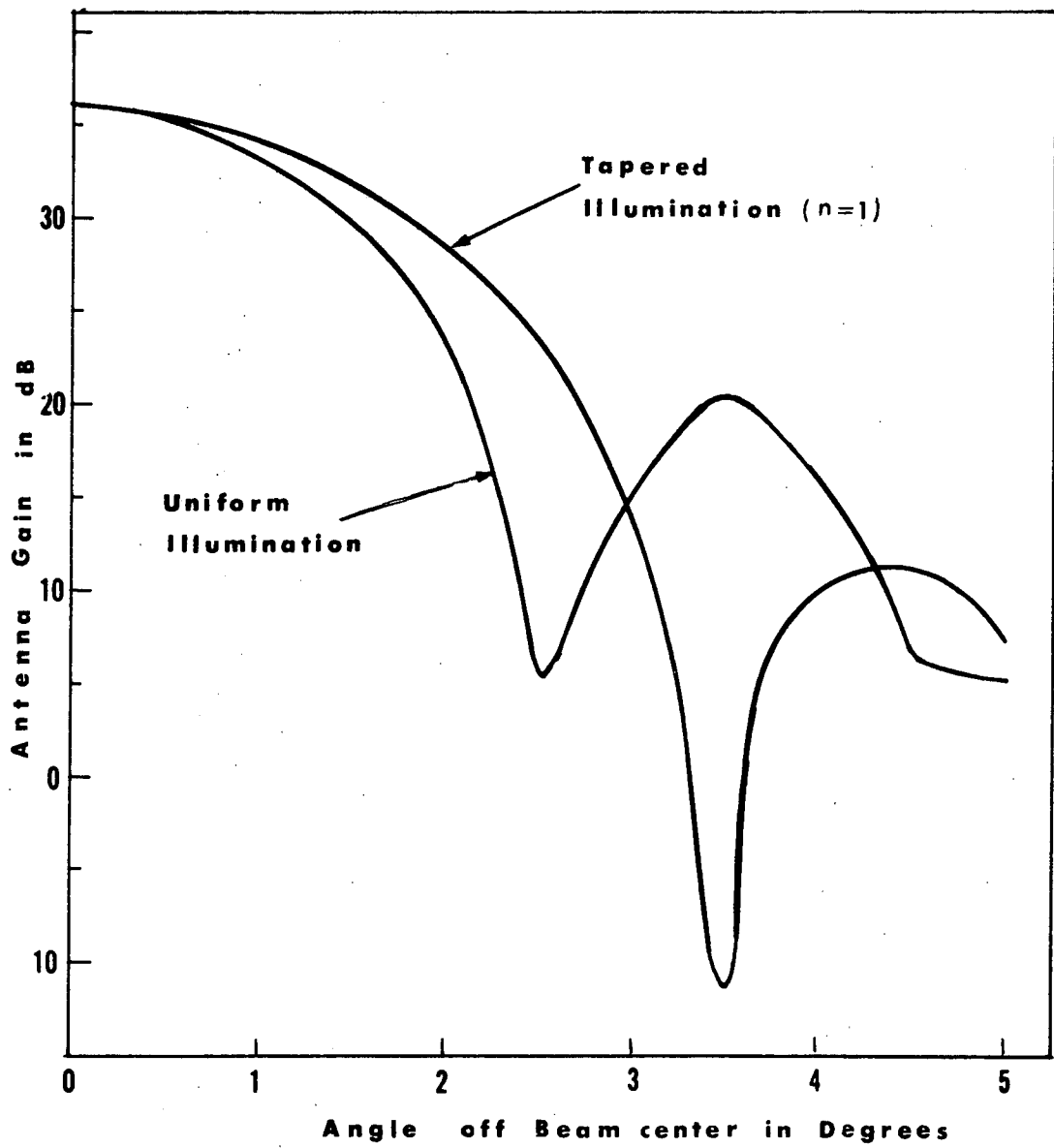
Figure 28. Antenna Gain Versus Angle Off Beam Center for Parabolic
Antenna with D/λ = 27.

(C/T) = carrier-to-noise temperature ratio, in dBW/°K.

TP = Transmitter output power, in dBW.

SNT = System noise temperature, in dB/°K.

TPL = Total propagation losses, in dB.

SAG = Satellite antenna gain, in dB.

RAG = Ground receiver antenna gain, in dB.

ULN = Uplink-noise, in dB.   (assumed 0.3 dB).

PL = Polarization losses, in dB.   (assumed 0.5 dB).

CL = Circuit losses, in dB.   (assumed 1.5 dB).

The values of (SNT + TPL) are the F(70,90) values indicated in Figure 26. The required picture quality boundaries are now determined as follows:

Figure 29 shows the design procedure at 12 GHz. The three contours of equal elevation angles (32.7°, 43.7°, and 55°)`, which are extrapolated to a larger scale from Figure 27 for the assumed satellite position are shown. The corresponding F(70,90) values are indicated on these. Now for a fine picture quality, the required (C/T) is -139.0 dBW/°K, and to obtain this at -3 dB antenna beam edge and 43.7° elevation angle, the satellite transmitter output power required may be computed from Equation (63) to be 27.78 dBW (600 watts/video channel). Assuming this, we may now rearrange Equation (63) for a fine picture quality as,

83
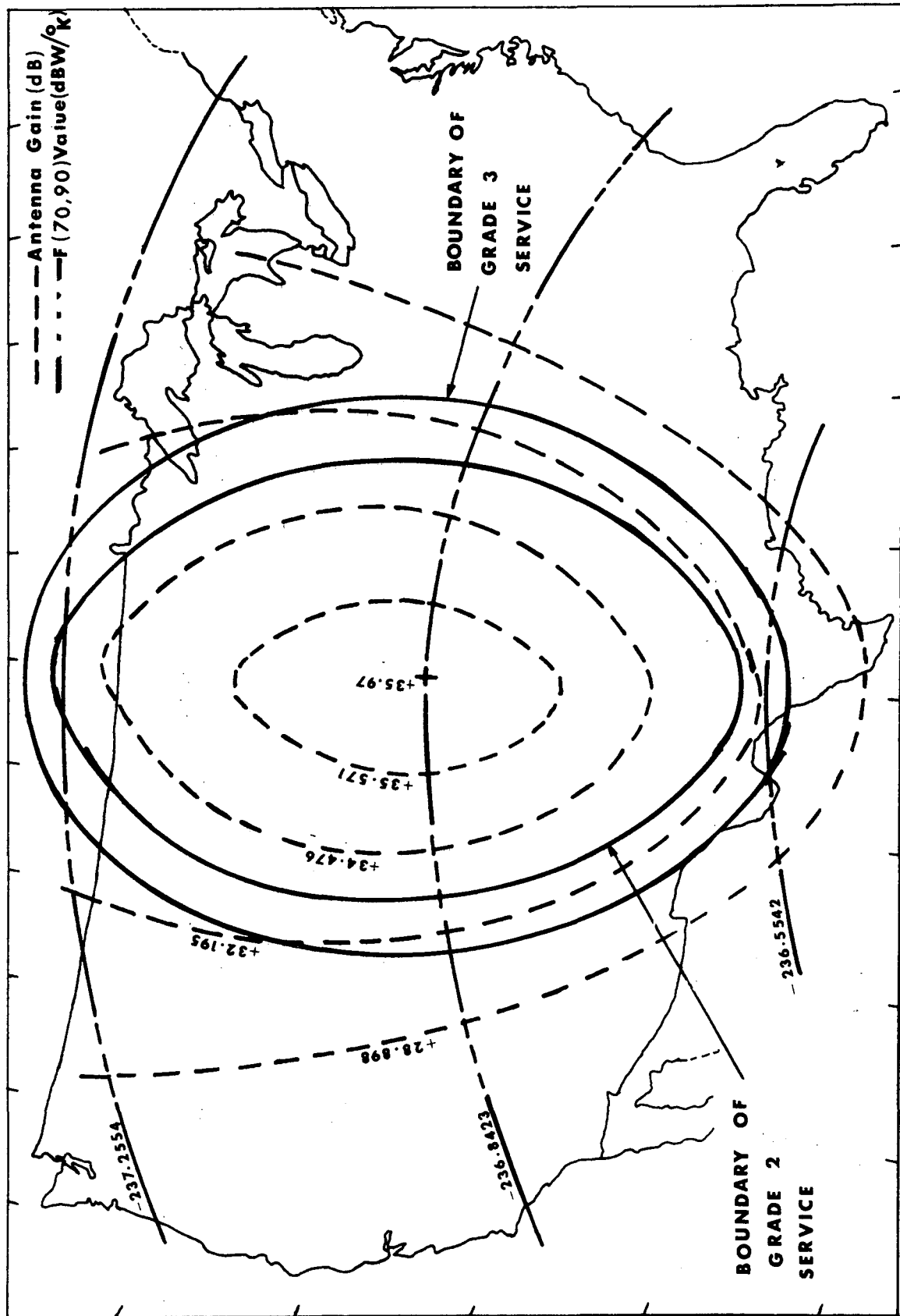
Figure 29. TVBS Picture Quality Contours for 12 GHz FM Transmission.

$$SAG + (SNT + TPL) = (-139.0 - 27.78 - 39.4 + 2.3)$$

$$SAG + (SNT + TPL) = -203.88 \text{ dBW/}^\circ\text{K.}$$

Now the positions on the map that result in a sum of antenna gain and F(70,90) values to be -203.88 dBW/°K are located and are joined by a closed contour. This represents the boundary of fine picture quality. Similarly the contour for passable picture quality is derived and shown in the same figure.

Figure 30 gives the same results for 2.5 GHZ, with a transmitter output power of 25.323 dBW (340 watts/video channel). It may be noted that effects of man-made noise in the metropolitan areas and of any special terrain or other features within the coverage area have been neglected. However, in an actual system, these effects may be considered in addition to the above discussed factors and the deterioration in the picture quality may be determined.
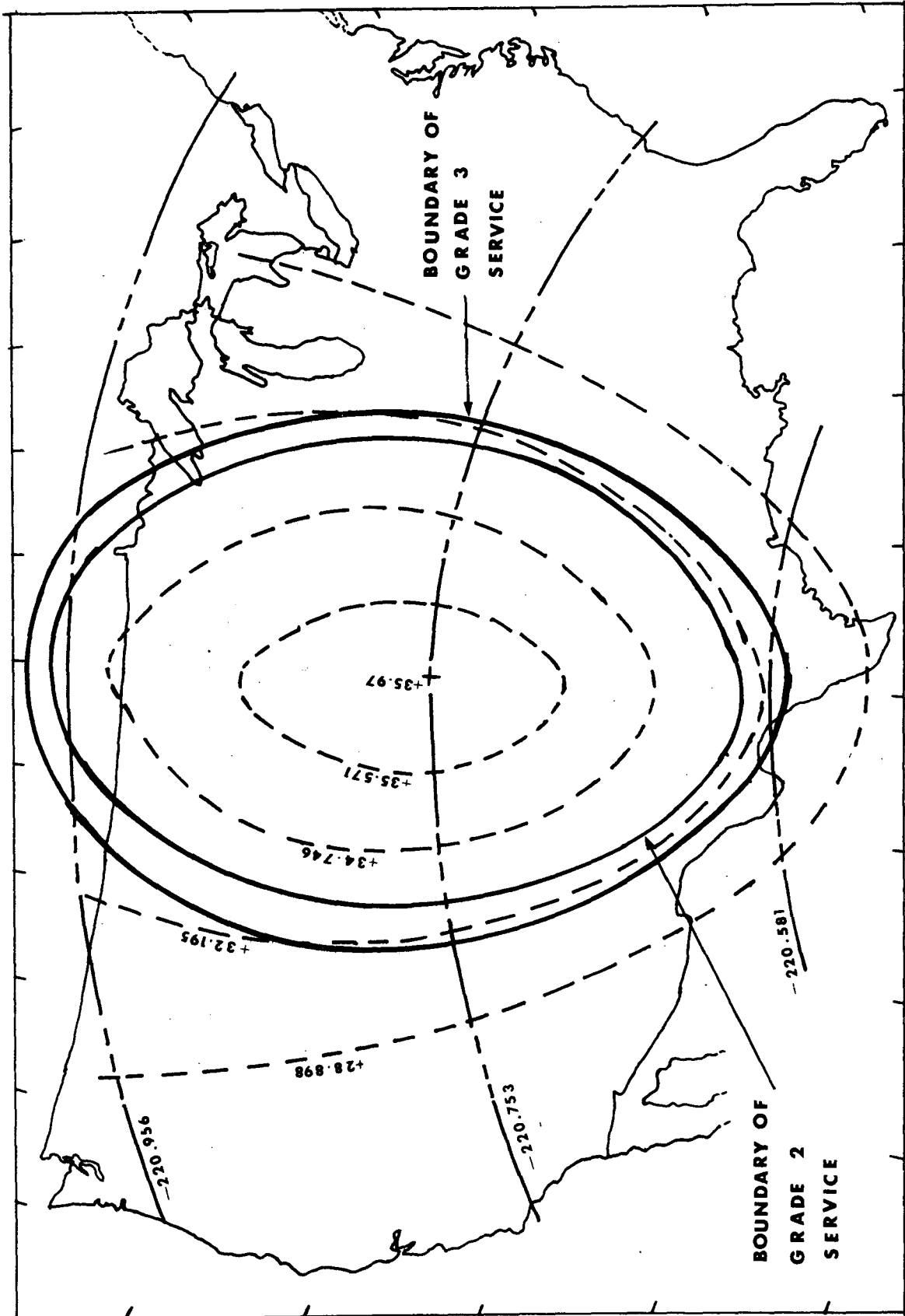
Figure 30. TVBS Picture Quality Contours for 2.5 GHz FM Transmission.

IX. CONCLUSION

The inevitable rise of so-called domestic communication satellites has already begun with the "molniya" system successfully operating in the U.S.S.R., and another system "Anik" to be implemented in Canada. Also the sudden action by the U.S. Federal Communications Commission to review the long dormant U.S. domestic proposals herald a totally new concept of communications. Both in United States and in India, special experiments are scheduled that will use a communication satellite to disseminate educational and health information [74]. The advantages of using communication satellites are undeniable, but careful planning is needed. In the present work, direct satellite television broadcast system is considered, assuming that such a system is feasible in the near future. High power spaceborne TV transmitter design and the development of a low cost, low noise ground receiver for domestic reception are the two most important problems that need to be solved for the implementation of a TVBS System. It is expected that if the technology development is continued at the present rate, the TVBS may become a reality in the 1975-85 period.

However, the most important contribution of this study has been the statistical analysis of propagation characteristics at 12 GHz. These results are extremely useful in the design of any communication satellite system in the temperate regions of the world.

Lastly, it may be mentioned that the satellite transmitter power requirements may be very much reduced, if the principle of phase-locked-loop is accepted for the ground receiver. However, much more work needs to be done in this field, before the economic and other aspects may be discussed.

2

BIBLIOGRAPHY

1. J. Jansen, P. L. Jordan, et.al. TRW Systems group, "Television Broadcast Satellite Study," Prepared for NASA, Contract NAS3-9707, October 1969.

2. Final Report, Communications and Systems, Incorporated, "Satellite Communications Systems, Technological Studies and Investigations," Prepared for NASW-1216, January 1969.

3. Report, General Electric Company, "Television Broadcast Satellite Study, Research and Technology Implications Report," Volumes I, II and III, Prepared for NASA, Contract NAS3-9708, August 1967-January 1969.

4. Report, Computer Sciences Corporation, "Satellite Communication Systems, Studies and Investigations," Prepared for NASA, Contract NAS5-11672, February 1971.

5. Application of MCI Lockheed Satellite Corporation for a "Domestic Communications Satellite System," before the Federal Communications Commission, Volumes I through IV, February 1971.

6. Final Report, Atlantic Research, "Technical and Cost Factors that Affect Television Reception From a Synchronous Satellite," Prepared for NASA, Contract NASW-1305, January 1966.

7. Eugene V. Shaparenko, Editor, The Saint Project, NASA-STANFORD UNIVERSITY Summer Training Program in Systems Engineering, August 1967.

8. Report, General Dynamics, "Television Broadcast Satellite Study,' Volumes I through V, Prepared for NASA, Contract NAS8-21036, December 1970.

9. Report, Meghdoot, A Proposal for a Study of an Indian Domestic Satellite System, Prepared for the Government of India, by Northrop Page Communications Engineers, January 1969.

10. L. H. Bedford, "Television by Satellite," The Radio and Electronic Engineer, pp. 273-283, November 1968.

11. P. J. Colburn, D. M. Squires and M. O'Hagan, "Television Broadcasting by Synchronous Satellite," The Aeronautical Journal of the Royal Aeronautical Society, Volume 73, pp. 273-283, April 1969.

12. K. G. Freeman, R. N. Jackson, P. L. Mothersole, and S. J. Robinson," Some Aspects of Direct Television Reception from Satellites," Proc. IEEE, Volume 117, Number 3, pp. 515-520, March 1970.

13. Q. B. McClannan and G. P. Heckert, "A Satellite System for CATV," Proc. IEEE, Volume 58, Number 7, pp. 987-1001, July 1970.

14. J. L. Hult, "Satellites and Technology for Communications: Shaping the Future," Paper presented for the International Symposium on Satellite Communication, at Zurich, Switzerland, April 24-27, 1968.

15. J. L. Hult, "The Promise of UHF Satellites for Mobile Services," Paper prepared for the Technical Symposium on Navigation and Positioning, hosted by the U. S. Army Electronics Command at Fort Mannouth, N. J. on 23-25, September 1969.

16. J. L. Hult, "Broadcast Opportunities with Satellites and CATV, and Their Control in the Public Interest," Paper prepared for the Seventh Space Congress, "Technology--Today and Tomorrow" at Cocoa Beach, Florida, April 22-24, 1970.

17. R. P. Haviland, "Why Space Broadcasting?" IEEE Spectrum, pp. 86-91, February 1970.

18. Lloyd Harrison et.al., "Canadian Domestic Satellite (TELESAT), A General Description," Paper presented at the International Conference on Communications, Montreal, June 1971.

19. J. Almond and R. M. Lester, "Communications Capability of the Canadian Domestic Satellite System," Paper presented at the International Conference on Communications, Montreal, June 1971.

20. J. Almond, "A Review of the Plans and Progress of the Initial Canadian Domestic Satellite Communication System," Paper presented at EASCON'71 Conference, Washington, October 1971.

21. E. T. Lipscomb, "High Power Spaceborne TV Transmitter Design Trade Offs for the 1970-1985 Period," AIAA paper no. 70-434, 3rd Communications Satellite Systems Conference, Los Angeles, California, April 6-8, 1970.

22. "Engineering Aspects of Television Allocations," Report of the TASO to the FCC, Volume I--March 1959, Volume II--June 1960.

23. J. H. Van Vleck, "The Absorption of Microwaves by Oxygen," Phys. Rev. Volume 71, #7, pp. 413-424, April 1947.

24. J. H. Van Vleck, "The Absorption of Microwaves by Uncondensed Water Vapor," Phys. Rev. Volume 71, #7, pp. 425-433, April 1947.

25. Vincent Falcone, Jr., "Calculations of Apparent Sky Temperature at mm Wave Lengths," Radio Science, Vol. I, No. 10, pp. 1205-1209, October 1966.

26. B. R. Bean and R. Abbott, "Oxygen and Water Vapor Absorption of Radio Waves in the Atmosphere," Geofisica Pura E Applicata, Vol. 37, pp. 127-144, 1957.

27. B. R. Bean and E. J. Dutton, "Radio Meteorology," National Bureau of Standards Monograph 92, March 1966.

28. G. E. Becker and S. H. Autlet, "Water Vapor Absoprtion of Electro-Magnetic Radiation in the cm Wavelength Range," Phys. Rev., Vol. 70, No. 5 and 6, pp. 300-307, 1946.

29. R. H. Dicke, R. Beringer, R. L. Kyhl, and A. B. Vane, "Atmospheric Absorption Measurements with a Microwave Radiometer," Phys. Rev., Vol. 70, NAS5 and 6, pp. 340-348, 1946.

30. J. O. Artman and J. P. Gordon, "Absorption and Temperature in Oxygen and Water Vapor," Phys. Rev. Vol. 96, p. 1237, 1954.

31. A. W. Straiton and C. W. Tolbert, "Anomalies in the Absorption of Radio Waves by Atmospheric Gases," Proc. IRE, pp. 898-903, May 1960.

32. E. E. Altshuler, V. J. Falcone, Jr., and K. N. Wulfsberg, "Atmospheric Effects on Propagation at mm Wavelengths," IEEE Spectrum, Vol. 5, pp. 83-90, July 1968.

33. B. C. Blevis, R. M. Dohoo, and McCormick, "Measurement of Rainfall Attenuation at 8 and 15 GHz," IEEE Trans. on Ant. and Propagation, Vol. AP-15, pp. 394-403, May 1967.

34. L. V. Blake, "Curves of Atmospheric Absorption Loss for Use in Radar Calculation," Report 5601, Naval Research Lab, March 1961.

35. B. R. Bean, "Attenuation of Radio Waves in the Troposphere," Advances in Radio Research, Academic Press, 1964, pp. 121-156.

36. J. P. Castelli, "Seasonal Atmospheric Attenuation Measurements," Radio Science, Vol. 1 (New Series) No. 10, pp. 1202-1205, October 1966.

37. Andre Benoit, "Signal Attenuation due to Neutral Oxygen and Water Vapor, Rain and Clouds," Microwave Journal, pp. 73-80, November 1968.

38. E. R. Westwater, " Ground-based Passive Probing using the Microwave Spectrum of Oxygen," J. Nat. Bur. Std. Radio Science, Vol. 69D, p. 1201, 1965.

39. C. C. I. R., Programmers d'Etudes 191(V) et 192(V), Documents de la xe Assemblée pléniére, Vol. II, Propagation, Rapport 234, Influence des Régions non-ionisées de l'Atmosphère sur la Propagation des ondes, U. I. T., Genéve, 1963.

40. K. L. S. Gunn and T. W. R. East, "The Microwave Properties of Precipitation Particles," Journal Royal Meteorological Society, Vol. 80, pp. 522-545, 1954.

41. R. L. Mitchell, "Some Applications of Milli-meter Waves in Atmospheric Research," Report for U. S. Air Force under Contract No. AF04 (695) -669.

42. J. W. Ryde, "The Attenuation and Radar Echoes Produced at cm Wavelengths by Various Meteorological Phenomena," Meteorological Factors in Radio Wave Propagation, The Physical Society (London), pp. 169-188, 1946.

43. Erwin Mondre, "Atmospheric Effects on mm Wave Communication Channels," Report X-733-70-250, Goddard Space Flight Center, Greenbelt, MD, March 1970.

44. D. Atlas, V. G. Plank, W. H. Paulsen, A. C. Chmela, J. S. Marshall, T. W. R. East, K. L. S. Gunn and W. Hirshfield, "Weather Effects on Radar," Geophysical Research Directorate, Air Force Survey in Geophysics, No. 23, 1952.

45. G. Mie, "Beitraege Zur Optik trüber Medien, Speziell Kolloidarer Metallösungen," Ann der Phys., Vol. 25, pp. 377-445, March 1908.

46. J. A. Stratton, "Electromagnetic Theory," New York, McGraw Hill, 1941, pp. 563-573.

47. J. W. Ryde, "Echo Intensity and Attenuation Due to Clouds, Rain, Hail, Sand and Dust Storms at cm Wavelengths," Rept 7831, General Electric Company Research Labs, Wembley, England, October 1941.

48. J. W. Ryde and D. Ryde, "Attenuation of cm Waves by Rain, Hail and Clouds," Rept. 8516, General Electric Co. Research Labs, Wembley, England, August 1944.

49. J. W. Ryde and D. Ryde, "Attenuation of cm and mm Waves by Rain, Hail, Fogs and Clouds," Rept 8670, General Electric Co. Research Labs, Wembley, England, May 1945.

50. R. G. Medhurst, "Rainfall Attenuation of cm Waves: Comparison of Theory and Measurement," IEEE Trans. on Ant. and Propagation, Vol. AP-13, pp. 550-564, July 1965.

51. J. A. Saxton, "The Anomalous Dispersion of Water at Very High Radio Frequencies: Part II--Relation of Experimental Observations to Theory," 1946 Conf. Rept. on Meteorological Factors in Radio Wave Propagation, The Physical Society (London), pp. 292-306, 1946.

52. J. O. Laws and D. A. Parsons, "The Relation of Raindrop Size to Intensity," Trans. Am. Geophysical Union, Vol. 24, pp. 432-460, 1943.

53. J. S. Marshall and W. McK. Palmer, "The Distribution of Rain Drops with Size," Journal of Meteorology, Vol. 5, pp. 165-166, August 1948.

54. V. N. Kelkar, "Size Distribution of Raindrops Pt. III," Indian J. Met. Geophys. No. 4, p. 553, 1961.

55. R. K. Crane, "Propagation Phenomena Affecting Satellite Communication Systems Operating in the cm and mm Wavelength Bands," Proc. IEEE, Vol. 59, No. 2, pp. 173-188, February 1971.

56. K. N. Wulfsberg and E. E. Altshuler, "Rain Attenuation at 15 and 35 GHz," IEEE Trans. on Ant. and Propagation, Vol. AP-20, No. 2, pp. 181-187, March 1972.

57. S. L. Godard, "Propagation of cm and mm Wavelengths Through Precipitation," IEEE Trans. on Ant. and Propagation, Vol. AP-18, No. 4, pp. 530-534, July 1970.

58. J. D. Greer, Agricultural Research Service, Holy Springs, Miss. Annual Report 1971. (Personal Communication from Dr. Parsons).

59. S. D. Robertson and A. P. King, "The Effect of Rain upon the Propagation of Waves in the 1- and 3- cm Regions," Proc. IRE, Vol. 34, pp. 178-180, April 1946.

60. D. C. Hogg, "Path Diversity of mm Waves Through Rain," IEEE Trans. on Ant. and Prop.,Vol. AP-15, pp. 410-415, May 1967.

61. S. D. Hathaway and H. E. Evans, "Radio Attenuation at 11 GHz and Implications Affecting Relay System Engineering," B.S.T.J., Vol. 38, pp. 73-97, January 1959.

62. H. H. Koelle, Ed., "Handbook of Astronautical Engineering," McGraw Hill, 1961, p. 16.

63. L. J. Ippolito, "mm Wave Propagation Measurements from the ATS-V," IEEE Trans. on Ant. and Propagation, Vol. AP-18, No. 4, pp. 189-205, July 1970.

64. L. J. Ippolito, "Effects of Precipitation on 15.3 and 31.65 GHz Earth-Space Transmissions with ATS-V Satellite," Proc. IEEE, Vol. 59, pp. 189-205, February 1971.

65. W. Holzer, "Atmospheric Attenuation in Satellite Communications," The Microwave Journal, pp. 119-125, March 1965.

66. Chandra Sekhar, Radiative Transfer, Dover Publications, New York, 1960.

67. K. N. Wulfsberg, "Sky Noise Measurements at mm Wave Lengths," Proc. IEEE, pp. 321-322, March 1964.

68. D. C. Hogg, "Effective Antenna Temperatures Due to O_2 and Water Vapor in the Atmosphere," J. App. Phys., Vol. 30, pp. 1417-1419. September 1959.

69. F. A. Berry, Jr., E. Bollay and N. R. Beers, "Handbook of Meteorology," McGraw-Hill Book Company, Inc., 1945, p. 70.

70. B. J. Mason, "Clouds, Rain and Rainmaking," University Press, Cambridge, 1962.

71. N. H. Fletcher, "The Physics of Rainclouds," University Press, Cambridge, 1962.

72. H. E. Bussey, "Microwave Attenuation Statistics Estimated from Rainfall and Water Vapor Statistics," Proc. IRE, Vol. 38, pp. 781-785, July 1950.

73. CCIR, XIIth Plenary Assembly CCIR Documents for Consideration at February Geneva Meeting, New Delhi, 1970, Doc. XI/1046-E.

74. Alexander A. McKenzie, "What is up in Satellites," IEEE Spectrum, Vol. 9, pp. 16-27, May 1972.

APPENDIX A

COMPUTER PROGRAM
FOR STATISTICAL ANALYSIS OF
ATMOSPHERIC EFFECTS ON SATELLITE
TRANSMISSION AT 12 GHz

```
C          STATISTICAL ANALYSIS OF ATMOSPHERIC ATTENUATION
          DIMENSIONTHETD(8),ALBAN(365,6),AG(365,8),AW(365,8),
         *AT(365,8),TS(365,8),BC(365,8),TE(365,8),MEANAT(8),
         *AP(365,8),ATSD(8),TEMEAN(8),TESD(8)
          REAL MEANAT,KW
C          READ ELEVATION ANGLE
          READ(5,99) (THETD(L),L=1,8)
   99 FORMAT(8F10.1)
C          READ   CLIMATOLOGICAL   DATA
          DO 3 I=1,365
          READ(5,1) (ALBAN(I,J),J=1,6)
    1 FORMAT(6F5.0)
          WRITE(6,2000) I
 2000 FORMAT(' ',I5)
    3 CONTINUE
          DO 101 L=1,8
          THETA=THETD(L)*3.141593/180.
          DO 2 I=1,365
C          COMPUTE ATTENUATION DUE TO OXYGEN AND WATER VAPOR
          RHO=ALBAN(I,1)
          RO=6378.
          RV=10.
          R=SQRT((RO**2)*((SIN(THETA))**2)+RV*(2.*RO+RV))
         *-RO*SIN(THETA)
          AG(I,L)=(8.5E-3+5.28E-4*RHO)*R
C          COMPUTE CLOUD ATTENUATION
          T=ALBAN(I,3)
          ROEW=ALBAN(I,4)
          RW=ALBAN(I,5)
          F=12.
          AO=-6.866
          B=1.95
          M=4.5E-3
          KW=(F**B)*EXP(AO*(1.+M*T))
          AW(I,L)=KW*ROEW*RW/SIN(THETA)
C          CALCULATE ATTENUATION DUE TO RAIN
          AKP=2.9E-2
          ALPHA=1.285
          PU=ALBAN(I,2)*25.4
          E=50.
          C=3./SIN(THETA)
          S=AMIN1(C,E)
          AP(I,L)=AKP*(PO**ALPHA)*S
          AT(I,L)=AG(I,L)+AW(I,L)+AP(I,L)
C          CALCULATE SKY NOISE TEMPERATURE
          TM=236.2+0.622*ALBAN(I,6)
          ALPHAT=10.**(AT(I,L)/10.)
          TS(I,L)=TM*(1.-1./ALPHAT)
```

```
      2 CONTINUE
        CALL SORT(AG,L)
        CALL SORT(AW,L)
        CALL SORT(AP,L)
        CALL SORT(AT,L)
        CALL SORT(TS,L)
        WRITE(6,54)
     54 FORMAT('1','WASHINGTON,DC')
        WRITE(6,56) THETD(L)
     56 FORMAT(' ',5X,'ELEVATION ANGLE=',F10.1)
        WRITE(6,11)
     11 FORMAT (' ',//,11X,'AG',20X,'AW',20X,'AP',20X,'AT',
       *20X,'TS',//)
        WRITE(6,12) (AG(I,L),AW(I,L),AP(I,L),AT(I,L),TS(I,L),
       *I=1,365)
     12 FORMAT(' ',5(5X,E15.7))
C         COMPUTE STANDARD DEVIATION OF TOTAL ATTENUATION
        MEANAT(L)=0.0
        DO 15 I=1,365
     15 MEANAT(L)=MEANAT(L)+(1./365.)*AT(I,L)
        DIFF=0.0
        DO 16 I=1,365
     16 DIFF=DIFF+((AT(I,L)-MEANAT(L))**2)
         ATSD(L)=SQRT(DIFF/365.)
C         COMPUTE STANDARD DEVIATION OF SYSTEM NOISE TEMP
        TEMEAN(L)=0.0
        DO 17 I=1,365
        TE(I,L)=TS(I,L)+1175.
        TE(I,L)=10.*ALOG10(TE(I,L))
     17 TEMEAN(L)=TEMEAN(L)+(1./365.)*TE(I,L)
        DIFF=0.
        DO 18 I=1,365
     18 DIFF=DIFF+((TE(I,L)-TEMEAN(L))**2)
        TESD(L)=SQRT((1./365.)*DIFF)
        WRITE(6,59) MEANAT(L),ATSD(L),TEMEAN(L),TESD(L)
     59 FORMAT(' ',//,3X,'MEAN OF AT=',E15.7,3X,'SD OF AT=',
       *E15.7,3X,'MEANOFTE=',E15.7,3X,'SD OF TE=',E15.7)
    101 CONTINUE
        STOP
        END
```

```
C      SUBROUTINE FOR CUMULATIVE DISTRIBUTIONS

       _____

       SUBROUTINE SORT(BC,L)
       DIMENSION BC(365,8)
       DO 2 J=1,364
       JP1=J+1
       K=J
       DO1 I=JP1,365
     1 IF(BC(K,L).LT.BC(I,L)) K=I
       CB=BC(K,L)
       BC(K,L)=BC(J,L)
       BC(J,L)=CB
     2 CONTINUE
       RETURN
       END
```